Cell Reports

Article

Mitochondrial Stress Restores the Heat Shock Response and Prevents Proteostasis Collapse during Aging

Graphical Abstract

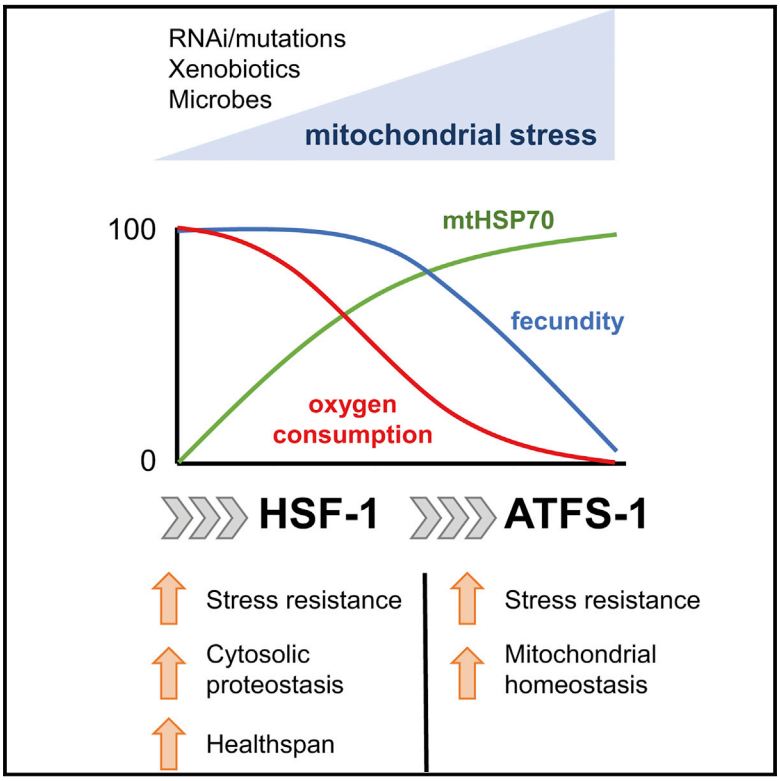

Authors

Johnathan Labbadia, Renee M. Brielmann, Mario F. Neto, Yi-Fan Lin, Cole M. Haynes, Richard I. Morimoto

Correspondence

j.labbadia@ucl.ac.uk (J.L.), r-morimoto@northwestern.edu (R.I.M.)

In Brief

Using the nematode *Caenorhabditis elegans*, Labbadia et al. demonstrate that low levels of mitochondrial stress caused by exposure to RNAi or xenobiotics can restore HSF-1 function with age, thereby maintaining cytosolic proteostasis, enhancing stress resistance, and prolonging healthspan, all without detrimental effects on development or reproduction.

Highlights

- Impaired mitochondrial function suppresses the programmed repression of the HSR
- Mitochondria regulate the collapse of stress resistance and cytosolic proteostasis
- The effect of mitochondria on stress resistance and proteostasis is regulated by HSF-1
- Mitochondrial "tuning" maintains cytoplasmic proteostasis without affecting fecundity

Labbadia et al., 2017, Cell Reports *21*, 1481–1494
November 7, 2017
https://doi.org/10.1016/j.celrep.2017.10.038

Cell Reports
Article

OPEN ACCESS
CellPress

Mitochondrial Stress Restores the Heat Shock Response and Prevents Proteostasis Collapse during Aging

Johnathan Labbadia,[1,3,*] Renee M. Brielmann,[1] Mario F. Neto,[1] Yi-Fan Lin,[2] Cole M. Haynes,[2] and Richard I. Morimoto[1,4,*]
[1]Department of Molecular Biosciences, Rice Institute for Biomedical Research, Northwestern University, Evanston, IL 60208, USA
[2]Department of Molecular, Cell and Cancer Biology, University of Massachusetts Medical School, Worcester, MA 01605, USA
[3]Institute of Healthy Ageing, Department of Genetics, Evolution and Environment, University College London, Darwin Building, Gower Street, London WC1E 6BT, UK
[4]Lead Contact
*Correspondence: j.labbadia@ucl.ac.uk (J.L.), r-morimoto@northwestern.edu (R.I.M.)
https://doi.org/10.1016/j.celrep.2017.10.038

SUMMARY

In *Caenorhabditis elegans*, the programmed repression of the heat shock response (HSR) accompanies the transition to reproductive maturity, leaving cells vulnerable to environmental stress and protein aggregation with age. To identify the factors driving this event, we performed an unbiased genetic screen for suppressors of stress resistance and identified the mitochondrial electron transport chain (ETC) as a central regulator of the age-related decline of the HSR and cytosolic proteostasis. Mild downregulation of ETC activity, either by genetic modulation or exposure to mitochondria-targeted xenobiotics, maintained the HSR in adulthood by increasing HSF-1 binding and RNA polymerase II recruitment at HSF-1 target genes. This resulted in a robust restoration of cytoplasmic proteostasis and increased vitality later in life, without detrimental effects on fecundity. We propose that low levels of mitochondrial stress regulate cytoplasmic proteostasis and healthspan during aging by coordinating the long-term activity of HSF-1 with conditions preclusive to optimal fitness.

INTRODUCTION

Old age is the primary risk factor for many human diseases, but the overarching principles and molecular mechanisms that drive aging remain poorly understood (López-Otín et al., 2013). Aging has long been thought of as a stochastic process that is characterized by the gradual accumulation of cell damage. However, recent evidence suggests that aging arises, at least in part, from programmed events early in life that promote reproduction (Labbadia and Morimoto, 2014).

In the nematode *Caenorhabditis elegans*, the ability to prevent metastable proteins from misfolding and aggregating fails early in adulthood, resulting in the appearance and persistence of protein aggregates in multiple tissues before animals have ceased reproduction (Ben-Zvi et al., 2009; David et al., 2010; Reis-Rodrigues et al., 2012; Walther et al., 2015).

Proteostasis is routinely maintained through the activity of constitutive and inducible stress response pathways. Among these, the transcription factor HSF-1 promotes the expression of molecular chaperones and enhances protein-folding capacity in the cytosol and nucleus through the heat shock response (HSR). During *C. elegans* adulthood, the HSR undergoes rapid repression as animals commence reproduction, thereby leaving cells vulnerable to environmental stress and proteostasis collapse well before overt signs of aging are distinguishable (Labbadia and Morimoto, 2015a; Shemesh et al., 2013). This suggests that precise regulatory switches actively repress the HSR early in life as part of programs that promote reproduction at the cost of proteostasis (Labbadia and Morimoto, 2015a). However, it remains unclear which molecular and physiological processes drive the repression of the HSR and the loss of stress resistance in adulthood, how environmental factors influence this, and whether maintenance of proteostasis can be uncoupled from reduced fecundity.

To this end, we performed an unbiased genetic screen to identify genes whose knockdown maintains resistance to thermal stress and prevents repression of the HSR in reproductively active adults. We identified the mitochondrial electron transport chain (ETC) as a robust determinant of the timing and severity of the decline in the HSR and show that mild mitochondrial stress increases HSF-1 binding at target promoters, maintains the HSR, and preserves proteostasis in reproductively active animals. These beneficial effects were achieved without the severe physiological defects typically associated with impaired mitochondrial function, suggesting that modulation of mitochondrial activity is a physiologically relevant determinant of the timing of repression of the HSR and cytosolic proteostasis collapse with age.

RESULTS

Complex IV Inhibition Increases Stress Resistance and Maintains the HSR with Age

The activity of the HSR and thermal stress resistance decline dramatically between day 1 and day 2 of adulthood in *C. elegans* (Labbadia and Morimoto, 2015a). To identify

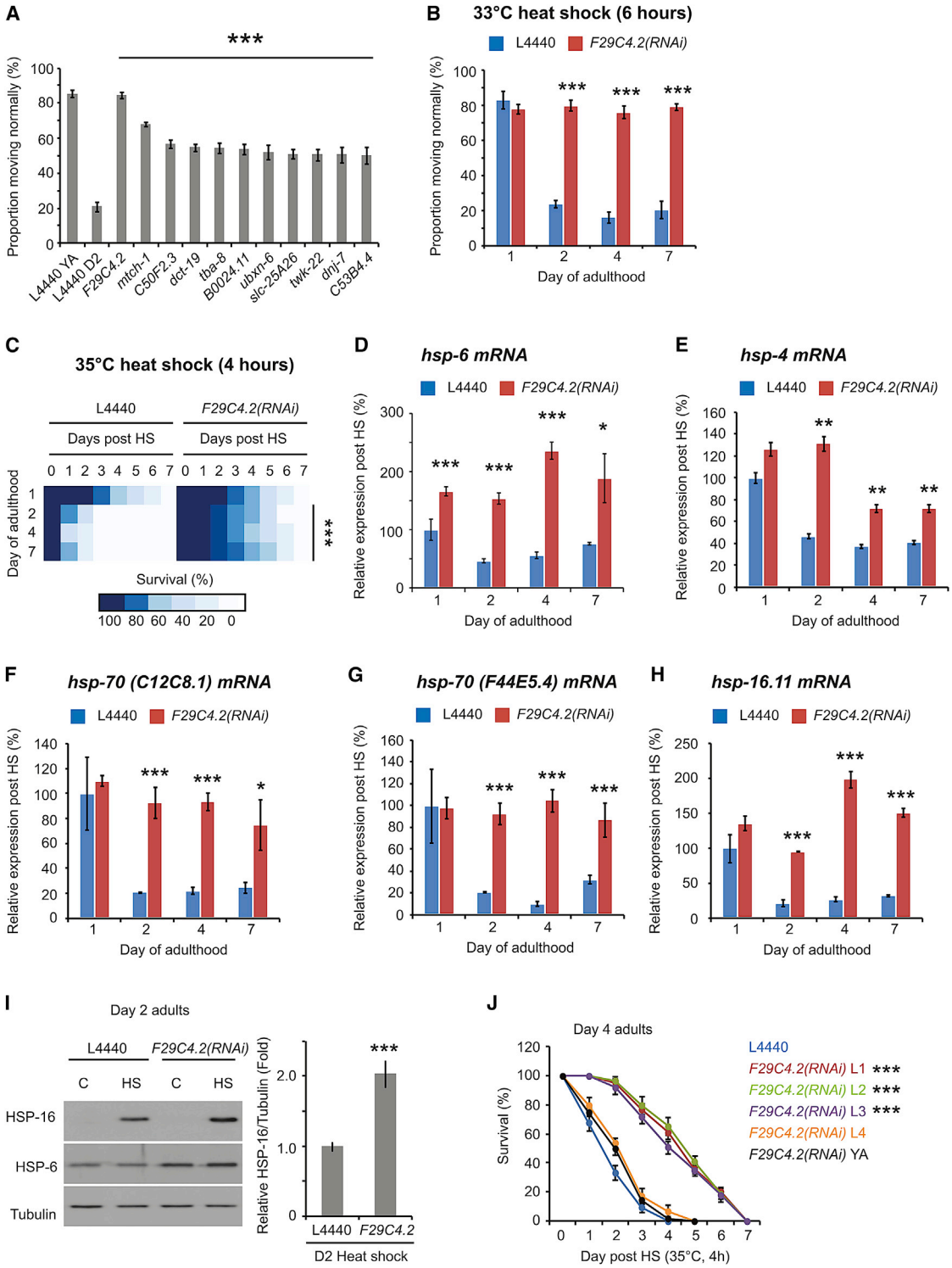

Figure 1. Complex IV Inhibition Increases Stress Resistance and Maintains the HSR in Reproductively Mature Adults

(A) RNAi clones that restore thermorecovery to at least 50% in reproductively active adults.

(B) Thermorecovery of L4440 or *F29C4.2(RNAi)*-treated worms 48 hr following heat shock (HS) (33°C, 6 hr) on solid NGM plates at different days of adulthood.

(C) Survival of L4440 or *F29C4.2(RNAi)*-treated worms following HS (35°C, 4 hr) on different days of adulthood. Related survival curves can be found in Figure S1.

(D–H) Relative expression of *hsp-6* (D), *hsp-4* (E), *hsp-70(C12C8.1)* (F), *hsp-70(F44E5.4)* (G), and *hsp-16.11* (H) relative to the housekeeping genes *rpb-2* and *cdc-42* in L4440 or *F29C4.2(RNAi)* treated animals following HS (33°C, 30 min) at different days of adulthood.

(legend continued on next page)

pathways that control the collapse of stress resistance, we performed an unbiased genome-wide RNAi screen for genes whose knockdown maintained resistance to thermal stress in reproductive (day 2, 24 hr post-vulva formation) adults (Figure S1A). At day 1 of adulthood (4 hr post-L4 molt), ~80% of animals move vigorously 48 hr after heat shock (HS) (Figure 1A). In contrast, on day 2, only 20% of adult animals exhibit normal movement after HS (Figure 1A). We identified 11 genes (Figure 1A; Table S1) whose knockdown restored stress resistance to at least 50% on day 2 of adulthood. Of these, knockdown of *F29C4.2* (a predicted cytochrome *c* oxidase subunit orthologous to human *COX6C* and previously identified in a paraquat resistance screen; Kim and Sun, 2007) fully restored stress resistance (Figure 1A). *F29C4.2(RNAi)* increased stress resistance through day 7 of adulthood (Figure 1B) and was effective in conferring protection against normally lethal stress conditions (Figures 1C and S1B), thus demonstrating that *F29C4.2* is a potent modifier of the decline in cellular robustness with age.

ETC disruption is associated with increased longevity and improved health through activation of the mitochondrial unfolded protein response (UPR^{mt}) (Yun and Finkel, 2014). Consistent with this, *F29C4.2(RNAi)* significantly increased basal expression of the canonical UPR^{mt} genes *hsp-6* and *hsp-60* on day 1 and day 2 of adulthood and strongly activated an *hsp-6*p::gfp reporter (Figures S1C–S1E). *F29C4.2(RNAi)* also enhanced *hsp-6* induction in response to HS on day 1 of adulthood and robustly maintained *hsp-6* inducible expression thereafter (Figure 1D). These results indicate that *F29C4.2(RNAi)* constitutively activates and enhances the responsiveness of the UPR^{mt} in adulthood, even before enhanced stress resistance is observed.

We next examined whether *F29C4.2(RNAi)* specifically augments the UPR^{mt} or has effects on the HSR and the endoplasmic reticulum UPR (UPR^{ER}), which both decline early in adulthood (Labbadia and Morimoto, 2015a; Taylor and Dillin, 2013). Basal expression of core cytosolic chaperones, canonical HSR genes, the ER inducible HSP70 homolog of the UPR^{ER}, and fluorescent reporters of the HSR or UPR^{ER} was not induced upon *F29C4.2(RNAi)* (Figures S1C–S1E). However, upon exposure to HS, the levels of *hsp-4, hsp-70(C12C8.1)*, *hsp-70(F44E5.4)*, and *hsp-16.11* were maintained from day 2 through day 7 of adulthood by *F29C4.2(RNAi)* (Figures 1E–1H). In keeping with the enhanced HSR in day 2 adults, HSP-16 protein levels were also increased 2-fold in *F29C4.2(RNAi)* animals compared to L4440 controls following HS (Figure 1I).

Consistent with reports from other groups (Kim et al., 2016; Yoneda et al., 2004), our data demonstrate that ETC perturbation activates the UPR^{mt} but does not constitutively activate the HSR or UPR^{ER}. Furthermore, we find that although *F29C4.2(RNAi)* results in activation of the UPR^{mt} during adolescence, enhanced induction of cell stress response genes is only observed in reproductively active adults, suggesting that ETC perturbation influences proteostasis-related pathways in a stage-specific manner.

Lifespan assurance and activation of the UPR^{mt} are dependent on changes in ETC activity during development (Dillin et al., 2002; Rea et al., 2007; Durieux et al., 2011). Therefore, we exposed animals to *F29C4.2(RNAi)* at distinct larval stages and measured stress resistance in post-reproductive adults. Exposure to *F29C4.2(RNAi)* in early development (L1–L3 stage) was sufficient to fully maintain stress resistance through day 4 of adulthood, whereas stress resistance was not enhanced in animals placed on *F29C4.2(RNAi)* from the L4 or young adult stages onward (Figure 1J). These findings suggest that, like lifespan extension and activation of the UPR^{mt}, the modulation of stress resistance with age is dependent on mitochondrial activity during development (Dillin et al., 2002; Rea et al., 2007; Durieux et al., 2011).

Disruption of Various Mitochondrial Pathways Enhances the HSR and Stress Resistance in Reproductively Mature Adults

Enhanced stress resistance is intimately linked to longevity, and it has been shown that RNAi of many mitochondria-associated genes extends lifespan (Bennett et al., 2014; Dillin et al., 2002; Houtkooper et al., 2013; Lee et al., 2003). Therefore, we asked whether *F29C4.2* was unique in its ability to enhance the HSR and maintain stress resistance. In our primary screen, several other genes encoding proteins with mitochondrial function (*cco-1, nuo-4, cyc-1, tomm-22*, and *mrps-5*) were identified but filtered out due to effects on development and/or fecundity. We therefore exposed animals to RNAi against subunits of complex I, complex III, and complex IV or against genes integral to mitochondrial import or mitochondrial protein synthesis and assessed stress resistance in reproductively mature adults. In addition, animals were exposed to RNAi against the AAA metalloprotease coding gene *spg-7*, which is known to induce the UPR^{mt} (Haynes et al., 2010; Yoneda et al., 2004). We corrected for developmental delay by assessing resistance to thermal stress in animals that were physiologically age matched (laying eggs for 24 hr prior to HS).

As expected, RNAi against all mitochondria-associated genes induced *hsp-6* expression (≥1.5-fold) at day 2 of adulthood (Figure S2A), but not the basal expression of HSR genes (Figure S2C). Upon exposure to heat stress, RNAi against subunits of complexes I, III, and IV or against *tomm-22* and *mrps-5* significantly increased stress resistance in reproductively active adults to an extent similar to that observed for *F29C4.2(RNAi)* (Figures 2A and S2B). However, RNAi against *dnj-21*, *tin-44*, *mrpl-1*, *mrpl-2*, and *spg-7* had little or no effect on stress resistance (Figures 2A and S2B). These data suggest

(I) Western blots of HSP-6, HSP-16, and tubulin at day 2 of adulthood in L4440- or *F29C4.2(RNAi)*-treated animals 24 hr following exposure to control or HS (33°C, 30 min) conditions at day 2 of adulthood. Levels of HSP-16 relative to tubulin were determined by densitometry, and the mean of 3 biological replicates is plotted. (J) Survival of animals following HS (35°C, 4 hr) on day 4 of adulthood following growth on L4440 or *F29C4.2(RNAi)* from the L1, L2, L3, or L4 larval stages or the young adult (YA) stage of life.

Unless stated, all values plotted are the mean of 4 biological replicates, and error bars denote SEM. Statistical significance was calculated by one-way ANOVA with Tukey pairwise analysis of groups (A), two-way ANOVA followed by Bonferroni correction and pairwise analysis of groups (B–H), two-tailed Student's t test (I), or two-way ANOVA followed by Bonferroni correction (J). *$p < 0.05$; **$p < 0.01$; ***$p < 0.001$.

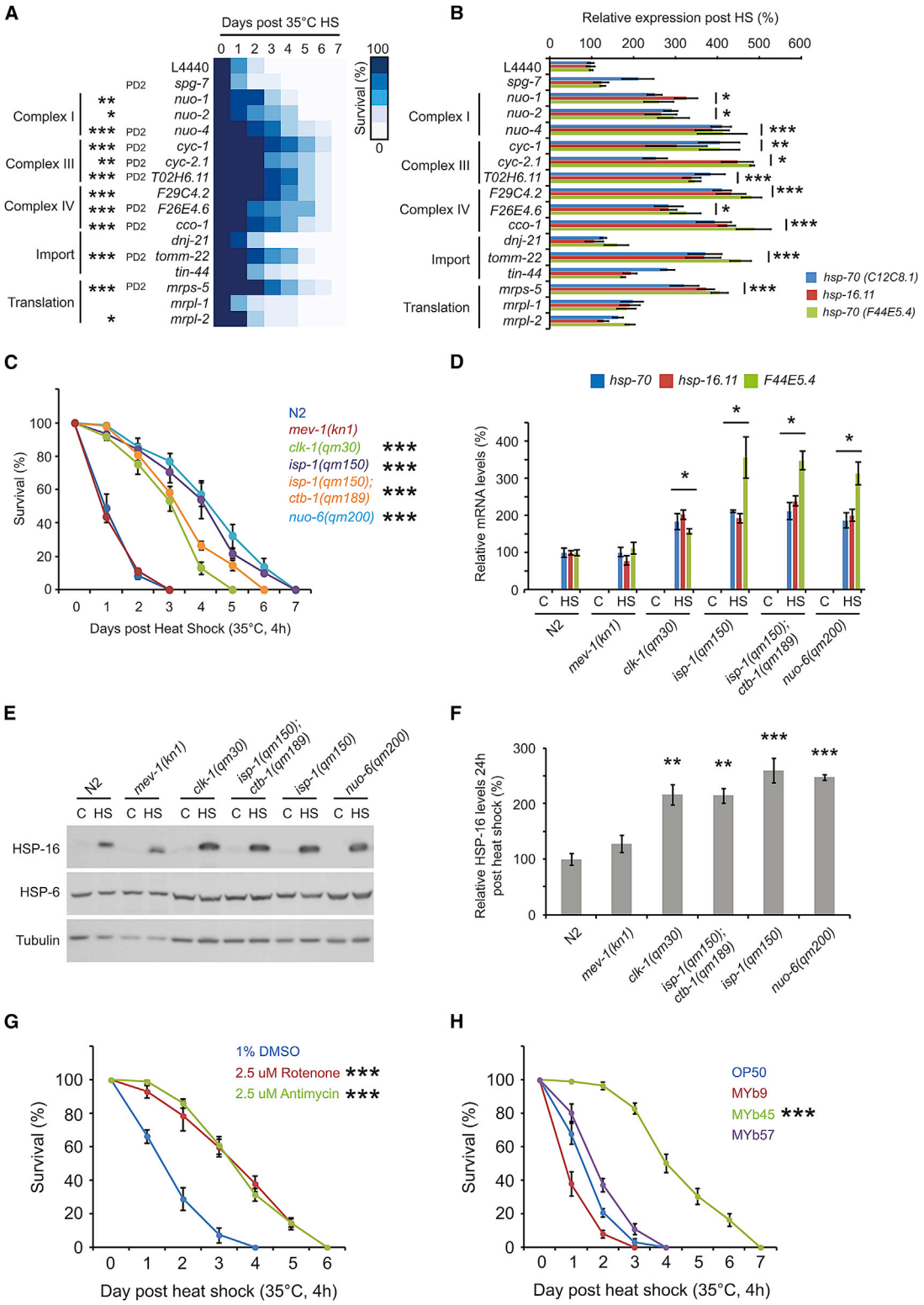

Figure 2. Multiple Forms of Mitochondrial Perturbation Maintain Stress Resistance and Enhance the HSR in Reproductively Mature Adults

(A) Survival following HS (35°C, 4 hr) at standard chronological day 2 of adulthood or physiological day 2 (PD2) of adulthood (animals were allowed to develop longer before HS to correct for delayed onset of egg-laying) in worms grown on empty vector control (L4440) or RNAi against mitochondria associated genes. Heatmap is plotted as the mean survival at different days post-HS for each condition. Related survival curves can be found in Figure S2.

(legend continued on next page)

that stress resistance can be enhanced in reproductively mature adults through perturbation of multiple mitochondrial pathways but that induction of mitochondrial stress is not always sufficient to maintain organismal stress resistance with age.

Consistent with their ability to enhance stress resistance, RNAi against subunits of complexes I, III, and IV as well as *tomm-22* and *mrps-5* also enhanced the expression of all three HSR genes to a similar extent as *F29C4.2(RNAi)*, while RNAi against *dnj-21*, *tin-44*, *mrpl-1*, *mrpl-2*, and *spg-7* had only modest effects on the expression of *hsp-70(C12C8.1)*, *hsp-70(F44E5.4)*, or *hsp-16.11* following HS (Figures 2A and 2B).

To extend beyond RNAi-based experiments, we examined activation of the HSR and stress resistance at day 2 of adulthood in animals with loss-of-function mutations in mitochondrial genes (Baruah et al., 2014; Feng et al., 2001; Lakowski and Hekimi, 1996; Walter et al., 2011; Butler et al., 2010). Long-lived *isp-1(qm150)*, *nuo-6(qm200)*, *isp-1(qm150);ctb-1(qm189)*, and *clk-1(qm30)* mutants, but not short-lived *mev-1(kn1)*, *gas-1(fc21)*, and *ucr-2.3(pk732)* mutants, all exhibited a greater than 3-fold increase in median survival, a 2- to 4-fold increase in the levels of *hsp-70*, *F44E5.4*, and *hsp-16.11* mRNA, and a 2- to 3-fold increase in levels of HSP-16 protein compared to wild-type worms following HS on day 2 of adulthood (Figures 2C–2F and S2D). This was not simply due to developmental delay in the onset of reproductive maturity or reduced fecundity, as *gas-1* and *ucr-2.3* mutants both exhibited an increased time to gravid adulthood (in the case of *ucr-2.3(pk732)* mutants, this was due to a delay in embryo formation once animals reached the first day of adulthood) and reduced brood size relative to N2 (Figures S2E and S2F).

In addition to genetic perturbation, mitochondrial stress is also induced by chemicals and some microbes (Liu et al., 2014). Therefore, we hypothesized that the mitochondria-mediated maintenance of stress resistance in adulthood could constitute a physiologically relevant adaptive response to conditions that compromise mitochondrial activity. To test this, we examined stress resistance in reproductively active adults exposed to complex I (rotenone) or complex III (antimycin) inhibitors during development. We found that growth on solid media containing 2.5 μM rotenone or 2.5 μM antimycin exclusively during development activated the UPR^{mt} without causing a pronounced developmental delay (Figure S2G) and increased stress resistance ~2-fold compared to vehicle-treated controls (Figure 2G).

Similarly, exposure to different microbes isolated from the natural environment of *C. elegans* has also been shown to activate the UPR^{mt} (Liu et al., 2014; Samuel et al., 2016). Using three bacterial strains proposed to inhabit the natural *C. elegans* microbiome (Dirksen et al., 2016), we found that growth on the *microbacterium* MYb45 robustly activated the UPR^{mt} (Figure S2G), whereas growth on the *achromobacter* strain MYb9 (increased brood size) or the *stenotrophomonas* strain MYb57 (no effect on brood size) did not activate the UPR^{mt} (Figure S2G). Consistent with the ability to induce mitochondrial stress, growth on MYb45, but not MYb9 or MYb57, enhanced stress resistance nearly 3-fold compared to animals grown on the standard laboratory *Escherichia coli* strain OP50 (Figure 2H).

Together, our data suggest that physiologically relevant conditions that cause mitochondrial stress can prevent the programmed loss of stress resistance that normally accompanies the commitment to reproductive maturity in early adulthood.

Physiological Defects Associated with Mitochondrial Perturbation Can Be Uncoupled from Beneficial Effects on the HSR and Stress Resistance

Although no developmental delay was observed, mitochondrial perturbation through *F29C4.2(RNAi)* did result in smaller animals, reduced brood size, and increased lethargy (Figures S3A and S3B). Previous studies have shown that dilution of ETC RNAi can significantly extend lifespan without many of the physiological defects observed upon full knockdown (Rea et al., 2007). Therefore, we adopted this approach with *F29C4.2(RNAi)* to determine whether the beneficial effects on stress resistance and the HSR could be separated from the deleterious consequences of ETC knockdown.

The level of *F29C4.2* knockdown was tuned by exposing animals to undiluted *F29C4.2(RNAi)* or to *F29C4.2(RNAi)* diluted between 2- and 1,000-fold with L4440 control bacteria (Figures S3A, S3C, and S3D). Knockdown of *F29C4.2* mRNA levels and activation of the UPR^{mt} were dose dependent (Figure S3D), and the severity of changes in body size, motility, and brood size were negatively correlated with levels of *F29C4.2* knockdown (Figure S3A). We found that a 5-fold dilution

(B) Expression of *hsp-70(C12C8.1)*, *hsp-70(F44E5.4)*, and *hsp-16.11* relative to the housekeeping genes *rpb-2* and *cdc-42* on day 2 of adulthood following HS (33°C for 30 min) in worms grown on L4440 or RNAi against mitochondria-associated genes.
(C) Survival following HS (35°C, 4 hr) on day 2 of adulthood in wild-type (N2) or mitochondrial mutant strains.
(D) Expression of *hsp-70(C12C8.1)*, *hsp-70(F44E5.4)*, and *hsp-16.11* relative to the housekeeping genes *rpb-2* and *cdc-42* on day 2 of adulthood following HS (33°C, 30 min) in wild-type and mitochondrial mutant animals.
(E) Western blots of HSP-6, HSP-16, and tubulin in wild-type and mitochondrial mutant animals 24 hr post-exposure to control or HS (33°C, 30 min) conditions on day 2 of adulthood.
(F) Levels of HSP-16 relative to tubulin on day 2 of adulthood in wild-type and mitochondrial mutant animals 24 hr post-exposure to control or HS (33°C, 30 min) conditions on day 2 of adulthood. Values plotted are the mean of 3 biological replicates.
(G) Survival following HS (35°C, 4 hr) on day 2 of adulthood in wild-type animals exposed to vehicle control (1% DMSO), 2.5 μM rotenone, or 2.5 μM antimycin until the late L4 stage.
(H) Survival following HS (35°C, 4 hr) on day 2 of adulthood in wild-type animals grown on OP50 *E. coli*, MYb9 *achromobacter*, MYb45 *microbacterium*, or MYb57 *stenotrophomonas*.
Unless stated, values plotted are the mean of 4 biological replicates, and error bars denote SEM. Statistical significance was calculated relative to L4440 by two-way ANOVA with Bonferroni correction (A and B), relative to N2 by two-way ANOVA with Bonferroni correction (C), one-way ANOVA with Tukey post-analysis pairwise comparison of groups (D and F), or two-way ANOVA with Bonferroni correction compared to 1% DMSO or OP50 control groups (G and H). *$p < 0.05$; **$p < 0.01$; ***$p < 0.001$.

of *F29C4.2(RNAi)* (hereafter referred to as *F29C4.2(0.2)(RNAi)*) maintained stress resistance to the same level as undiluted *F29C4.2(RNAi)* without significant reductions in motility or brood size and with only a modest (20%) reduction in body size (although the period of egg-laying was slightly extended) (Figures S3A–S3E). *F29C4.2(0.2)(RNAi)* resulted in a 50%–60% reduction in *F29C4.2* mRNA levels and a 30% reduction in the oxygen consumption rate (OCR) on day 2 of adulthood compared to 80% and 50% reductions, respectively, in undiluted *F29C4.2(RNAi)* animals (Figures 3A and 3B). The OCR increased 2-fold between day 1 and day 2 of adulthood in all treatment groups, likely due to growth and increased oocyte mass during this time period (Figure 3B). Similarly, ATP levels also increased 3- to 5-fold in L4440 and *F29C4.2(0.2)(RNAi)* animals during this time period but did not increase significantly in *F29C4.2(RNAi)* worms (Figure 3C). ATP levels were not altered compared to L4440 in *F29C4.2(RNAi)* or *F29C4.2(0.2)(RNAi)* animals on day 1 of adulthood. However, by day 2 of adulthood, ATP levels decreased by 80% and 30% in *F29C4.2(RNAi)* and *F29C4.2(0.2)(RNAi)* animals, respectively (Figure 3C). Crucially, despite milder effects on animal physiology, OCR, and ATP levels, *F29C4.2(0.2)(RNAi)* still resulted in increased expression of *hsp-6* and *hsp-60* (Figure S3F) and maintained stress resistance through day 15 of adulthood (Figure 3D).

Reactive oxygen species (ROS) generated by mitochondrial stress have been proposed to act as life-lengthening signaling molecules (Yang and Hekimi, 2010). Levels of general ROS, H_2O_2, and protein carbonylation were significantly increased following treatment with *F29C4.2(RNAi)* (Figures S3G–S3I), consistent with mitochondrial dysfunction (Segref et al., 2014). Conversely, animals grown on *F29C4.2(0.2)(RNAi)* exhibited smaller increase in ROS on day 1 and day 2 of adulthood and little to no difference in levels of H_2O_2 or protein carbonylation (Figures S3G–S3I), suggesting that maintenance of the HSR, enhanced stress resistance, and preservation of proteostasis do not require substantial increases in ROS levels and are not due to wide-scale oxidative damage to proteins (Figures S3G–S3I).

To determine whether increased stress resistance was still associated with an enhanced activity of stress response pathways, we exposed L4440 and *F29C4.2(0.2)(RNAi)* animals to HS at day 1 and day 2 of adulthood and quantified expression levels of HSR, UPR^{ER}, and UPR^{mt} genes. *F29C4.2(0.2)(RNAi)* did not constitutively activate the HSR or UPR^{ER} or lead to enhanced induction of these genes upon HS at day 1 of adulthood (Figures 3E–3G). Furthermore, although levels of the oxidative stress responsive gene *gst-4* are enhanced by elevated ROS and chronic mitochondrial perturbation (Schaar et al., 2015), we did not observe activation of a *gst-4p::gfp*-based reporter of the oxidative stress response or enhanced *gst-4* expression in response to heat stress by *F29C4.2(0.2)(RNAi).* Curiously, *gst-4* mRNA levels were significantly reduced in day 1 adults (Figure 3F and G), suggesting that while *F29C4.2(0.2)(RNAi)* results in reduced oxygen consumption, this is not associated with elevated *gst-4* expression, possibly because steady-state ROS levels are not dramatically increased (Figures S3G and S3H) and/or because the ability to express *gst-4* may be impaired. While *F29C4.2(0.2)(RNAi)* did not maintain the UPR^{ER} or oxidative stress response at day 2 of adulthood, the induction of HSR genes and HSP-16 protein levels were increased by 2- to 3-fold following HS on day 2 of adulthood (Figures 3E and 3J).

Repression of the HSR in reproductively active adults has been shown to be due to a reduced ability of HSF-1 to bind to target promoters and enhance transcription in response to HS (Labbadia and Morimoto, 2015a). Therefore we asked whether *F29C4.2(0.2)(RNAi)* could enhance the levels of HSF-1 and RNA polymerase II (Pol II) at HSR promoters using animals expressing a single copy of HSF-1::GFP (Li et al., 2016). HSF-1::GFP animals exhibit an enhanced HSR and stress resistance in response to *F29C4.2(0.2)(RNAi)* (Figures S3J and S3K). Furthermore, HSF-1 and RNA Pol II levels were increased ~2-fold at HSR promoters in *F29C4.2(0.2)(RNAi)* animals following HS at day 2 of adulthood (Figure 3H), without significant changes in the expression, stability, or nuclear localization of HSF-1 (Figures 3I, S3L, and S3M).

Our data demonstrate that mitochondrial stress can be "tuned" to enhance the HSR and prevent the age-related decline in stress resistance without the burden of severe physiological defects. This suggests that the influence of mitochondria on age-related changes in non-mitochondrial stress resistance pathways represents a physiologically relevant strategy by which cells and organisms use environmental cues to coordinate the onset of reproduction and the decline of stress responses with age.

Mitochondrial Stress Prevents the Age-Dependent Collapse of Cytosolic Proteostasis

Coincident with the rapid decline in stress resistance, proteostasis also collapses dramatically in multiple tissues during early *C. elegans* adulthood (Ben-Zvi et al., 2009; David et al., 2010). Therefore, we asked whether mild mitochondrial perturbation could prevent proteostasis collapse in the cytosol with age using animals expressing endogenous metastable proteins or exogenous aggregation prone proteins in intestinal cells or body wall muscle cells.

Animals expressing 44 polyglutamine (polyQ) residues fused to YFP (polyQ(44)::YFP) in intestinal cells (Mohri-Shiomi and Garsin, 2008; Prahlad and Morimoto, 2011) show diffuse polyQ44::YFP fluorescence throughout the intestine on day 1 of adulthood, the intensity and localization of which is unaltered by *F29C4.2(0.2)(RNAi)* (Figure S4C). However, by day 7 of adulthood, greater than 80% of the population exhibits large SDS insoluble polyQ aggregates in the proximal intestinal cells (Figures 4A–4C and S4C). Growth on *F29C4.2(0.2)(RNAi)* profoundly reduced the number of animals containing polyQ aggregates with age and almost completely suppressed the formation of SDS-insoluble polyQ aggregates in intestinal cells (Figures 4B and 4C) without affecting expression of the Q44::YFP transgene (Figure S4A). Although variable across samples, *F29C4.2(0.2)(RNAi)*-treated animals exhibited a trend toward increased levels of soluble polyQ protein on day 3 of adulthood, possibly due to impairments in protein turnover (Segref et al., 2014; Livnat-Levanon et al., 2014). However, this did not affect the ability to suppress aggregate formation with age (Figures 4B and S4D).

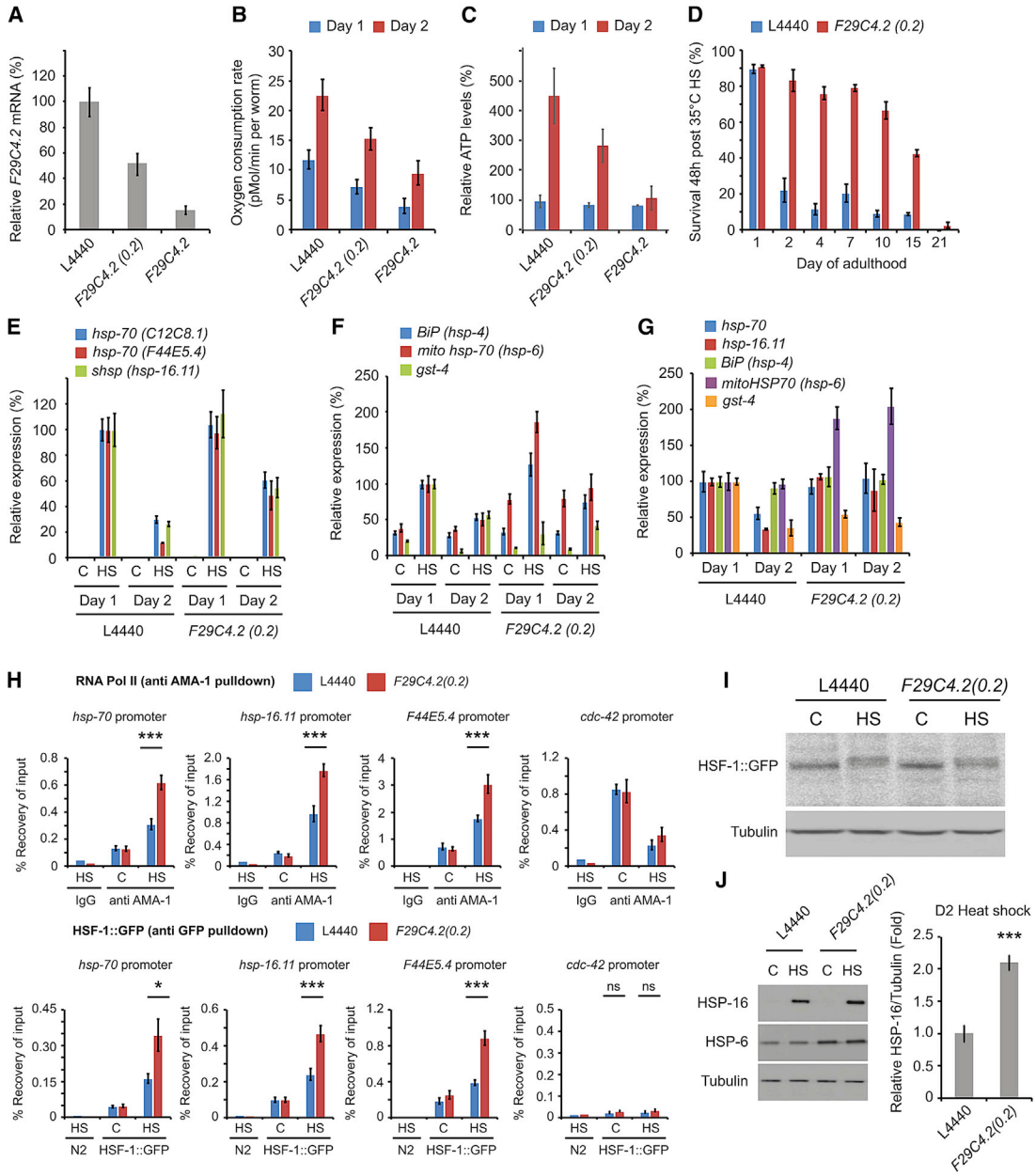

Figure 3. The Gross Physiological Defects Associated with Mitochondrial Perturbation Can Be Uncoupled from Enhanced Stress Resistance

(A) *F29C4.2* mRNA levels normalized to the house keeping genes *rpb-2* and *cdc-42* on day 2 of adulthood.

(B) Oxygen consumption rates at day 1 and day 2 of adulthood. Values plotted are the mean of 3 biological replicates.

(C) ATP levels at day 1 and day 2 of adulthood.

(D) Survival 48 hr following HS (35°C, 4 hr) on day 2 of adulthood.

(E–G) Expression of canonical (E) HSR (*C12C8.1, F44E5.4, hsp-16.11*) or (F) UPR^{ER} (*hsp-4*), UPR^{mt} (*hsp-6*), and oxidative stress response (*gst-4*) genes on day 1 and day 2 of adulthood following exposure to either control or HS (33°C, 30 min) conditions or (G) HS conditions alone. Expression of all genes was normalized to the housekeeping genes *rpb-2* and *cdc-42*.

(H) RNA polymerase II (AMA-1) (top) and HSF-1::GFP ChIP (bottom) followed by qPCR for *hsp-70*, *hsp-16.11*, *F44E5.4*, and *cdc-42* promoters in day 2 adults exposed to control or HS (33°C, 30 min) conditions.

(I) Western blots of HSF-1::GFP and tubulin in worms exposed to control or HS (33°C, 30 min) conditions on day 2 of adulthood. The slight shift in HSF-1 SDS-PAGE mobility corresponds to the well-documented hyperphosphorylation of HSF-1 following HS.

(J) Western blots of HSP-16, HSP-6, and tubulin at day 2 of adulthood 24 hr following exposure to control conditions or HS (33°C, 30 min) at day 2 of adulthood. Levels of HSP-16 relative to tubulin were calculated from 3 biological replicates.

Unless stated, all values plotted are the mean of 4 biological replicates, and error bars denote SEM. Statistical significance was calculated by two-way ANOVA with Bonferroni correction followed by pairwise analysis of groups (H) or two-tailed Student's t test (J). *$p < 0.05$; **$p < 0.01$; ***$p < 0.001$.

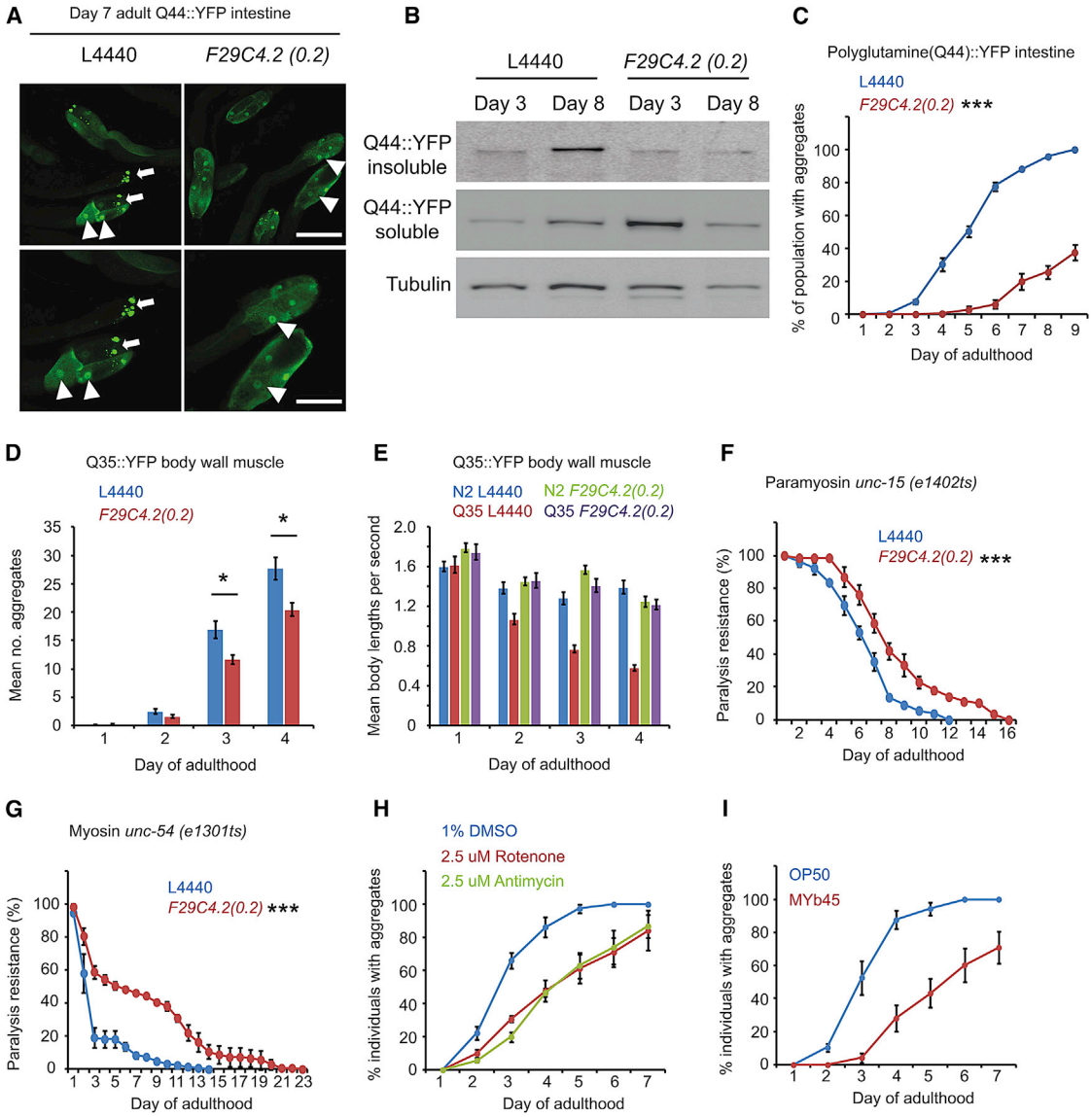

Figure 4. Mitochondrial Perturbation Suppresses Proteostasis Collapse in the Cytosol

(A) Representative images of the proximal intestine of worms expressing 44 polyglutamine (polyQ) residues fused to YFP (*vha-6p::polyQ(44)::yfp*) on day 7 of adulthood. Triangles indicate nuclei and arrows indicate polyQ aggregates. Scale bars represent 250 μM (top) and 100 μM (bottom).

(B) Western blots of insoluble and soluble Q44::YFP and tubulin at day 3 and day 8 of adulthood.

(C) Proportion of individuals exhibiting intestinal Q44::YFP aggregates at different days of adulthood.

(D) Number of Q35::YFP foci in body wall muscle cells of *unc-54p::polyQ(35)::YFP* animals at different days of adulthood.

(E) Motility of wild-type (N2) animals and animals expressing Q35::YFP in body wall muscle cells (*unc-54p::polyQ(35)::YFP)* at different days of adulthood.

(F and G) Age-related paralysis in animals expressing endogenous metastable (F) paramyosin (unc-15(e1402ts)) or (G) myosin (unc-54(e1301ts)).

Unless stated, all values were the mean of 4 biological replicates, and error bars denote SEM. Statistical significance was calculated by two-way ANOVA with Bonferroni correction. *$p < 0.05$; ***$p < 0.001$.

(H and I) Proportion of animals exhibiting intestinal Q44::YFP aggregates at different days of adulthood following growth on vehicle control, 2.5 μM rotenone, or 2.5 μM antimycin during development (L1 to late L4) (H) or growth on OP50 *E. coli* or MYb45 *microbacteria* (I).

Furthermore, *F29C4.2(0.2)(RNAi)* also suppressed polyQ(35)::YFP aggregation and toxicity in body wall muscle cells by 20% at day 3 and day 4 of adulthood without affecting expression of the Q35::YFP transgene (Figures 4D, 4E, and S4B), and it delayed the onset of paralysis at permissive temperatures in animals harboring destabilizing point mutations in the essential muscle proteins paramyosin (*unc-15ts*) or myosin (*unc-54ts*) (Figures 4F and 4G), suggesting that mitochondrial activity is a general determinant of the timing and severity of proteostasis collapse with age in different tissues.

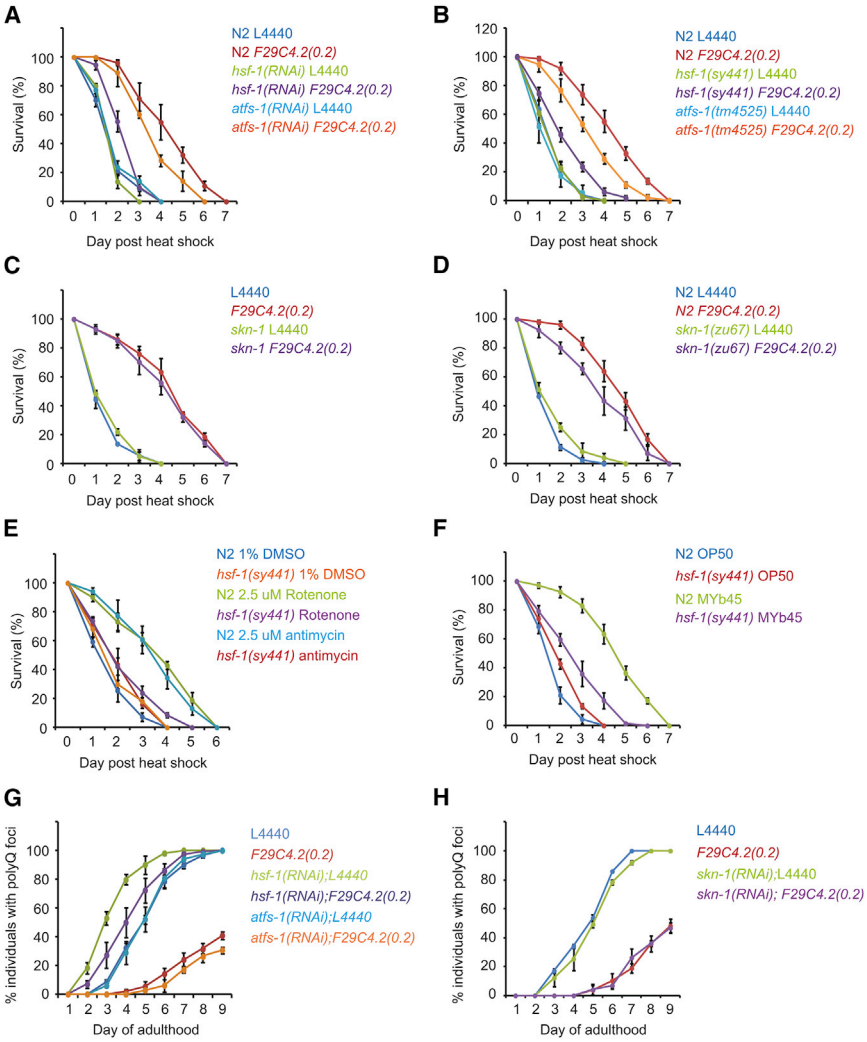

Figure 5. Mitochondrial Perturbation Enhances Stress Resistance and Maintains Proteostasis in an HSF-1-Dependent Manner

(A–D) Survival following HS (35°C, 4 hr) on day 2 of adulthood in animals grown on L4440 or *F29C4.2(0.2)* RNAi in the presence of (A) *hsf-1* or *atfs-1* RNAi, (B) *hsf-1(sy441)* or *atfs-1(tm4525)* loss of function mutations, (C) *skn-1* RNAi, or (D) a *skn-1(zu67)* loss of function mutation.

(E and F) Survival following heat shock (35°C, 4 h) on day 2 of adulthood in wild-type (N2) and *hsf-1(sy441)* mutant animals grown in the presence of (E) DMSO, rotenone, or antimycin until the late L4 stage or (F) OP50 or MYb45 bacterial strains until day 2 of adulthood.

(G and H) Proportion of Q44::YFP animals exhibiting intestinal polyQ aggregates at different days of adulthood after growth with (G) combinatorial L4440, *F29C4.2*, *hsf-1*, or *atfs-1* RNAi, or (H) combinatorial L4440, *F29C4.2*, or *skn-1* RNAi.

Unless stated, all values are the mean of 4 biological replicates, and error bars denote SEM.

Finally, consistent with their ability to increase stress resistance, exposure to rotenone, antimycin, or the *microbacterium* MYb45 reduced polyQ aggregation by 40%–50% at days 3–5 of adulthood (Figures 4H, 4I, and S4E) compared to control-treated animals. Although these effects were less profound than those observed with *F29C4.2(0.2)(RNAi)*, our data nevertheless suggest that mild mitochondrial stress from physiologically relevant xenobiotics and microbes can reset cytosolic proteostasis collapse with age.

Mitochondrial Perturbation Enhances Stress Resistance and Cytosolic Proteostasis in an HSF-1-Dependent Manner

Mitochondrial perturbation is primarily associated with activation of the UPR^{mt} and restoration of mitochondrial proteostasis. An important distinction shown here is that mitochondrial perturbation also maintains the HSR and cytosolic proteostasis with age. Given that the transcription factor HSF-1 is central to the HSR, stress resistance, and cytosolic proteostasis (Akerfelt et al., 2010; Li, Labbadia and Morimoto, 2017), we asked whether the beneficial effects of mitochondrial stress require HSF-1. Therefore, we examined survival following HS in animals exposed to L4440 or *F29C4.2(0.2)(RNAi)* in combination with *hsf-1(RNAi)* or *atfs-1(RNAi),* and in *hsf-1(sy441)* and *atfs-1(tm4525)* mutants that have a diminished HSR and UPR^{mt}, respectively (Bennett et al., 2014; Li et al., 2016; Nargund et al., 2015). Both RNAi-mediated knockdown and loss-of-function mutations in *hsf-1* and *atfs-1* severely dampened the ability of *F29C4.2(0.2)(RNAi)* to induce stress response genes and fluorescent reporters associated with the HSR and UPR^{mt}, thereby demonstrating that HSF-1 and ATFS-1 are essential for *F29C4.2(0.2)RNAi* to enhance the HSR and UPR^{mt}, respectively (Figures S5A–S5D).

Furthermore, while *F29C4.2(0.2)(RNAi)* significantly increased median survival following HS from 1.5 days to 4.1 days (Figure 5A), knockdown in the presence of either *atfs-1(RNAi)* or *hsf-1(RNAi)* reduced stress resistance by 25%, and 70%, respectively (Figure 5A). Similarly, *F29C4.2(0.2)(RNAi)*-mediated stress resistance was also decreased by 32% in *atfs-1(tm4525)* mutants and by 69% in *hsf-1(sy441)* mutants (Figure 5B), without affecting the efficacy of *F29C4.2* knockdown (Figure S5E). Likewise, disruption of the oxidative stress response through RNAi or a loss-of-function mutation of the transcription factor SKN-1 ((*skn-1(zu67)*) had only modest effects on stress resistance in *F29C4.2(0.2)(RNAi)* animals (Figures 5C and 5D). Our data therefore suggest that *atfs-1* and *skn-1* contribute only modestly to stress resistance in *F29C4.2(0.2)(RNAi)*-treated animals and that mild ETC perturbation promotes stress resistance predominantly through *hsf*-1 and the HSR.

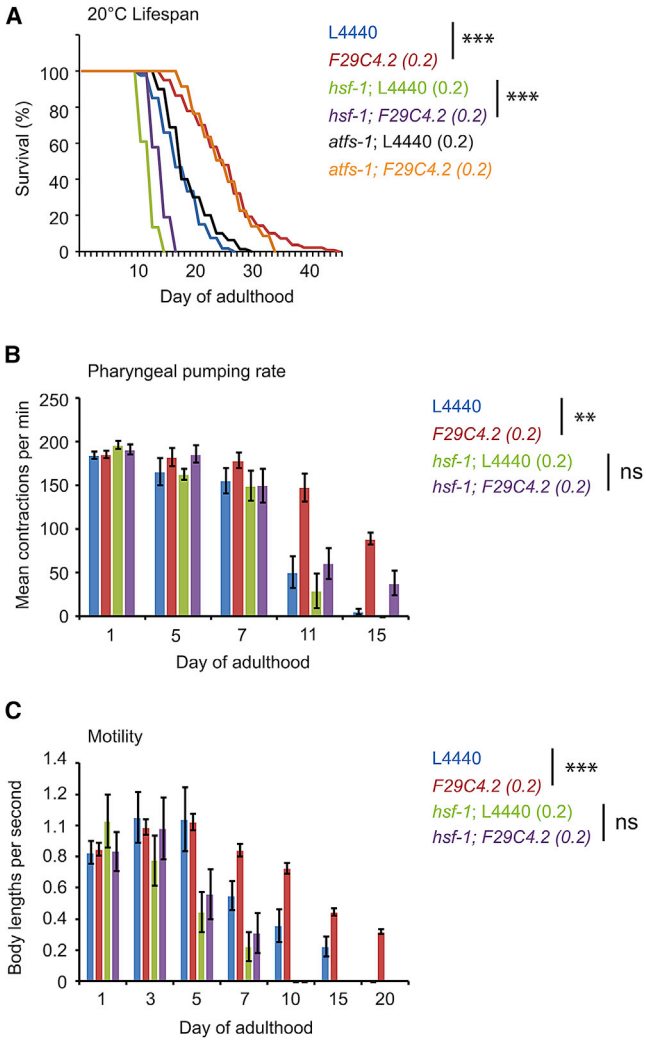

Figure 6. Mitochondrial Perturbation Maintains Somatic Health in an HSF-1-Dependent Manner

(A) Lifespan of wild-type worms grown on L4440 (n = 120), *F9C4.2(0.2)* (n = 129), *hsf-1*;L4440(0.2) (n = 97), *hsf-1;F29C4.2(0.2)* (n = 88), *atfs-1*; L4440(0.2) (n = 120), or *atfs-1; F29C4.2(0.2)* (n = 103) RNAi at 20°C. Median lifespans were 18, 28, 14, 16, 19, and 29 days, respectively. A second trial was also run and yielded highly similar results: L4440 (n = 81, 18 days), *F9C4.2(0.2)* (n = 82, 26 days), *hsf-1*;L4440(0.2) (n = 90, 14 days), *hsf-1;F29C4.2(0.2)* (n = 89, 16 days), *atfs-1*; L4440(0.2) (n = 80, 18 days), or *atfs-1; F29C4.2(0.2)* (n = 93, 28 days).

(B and C) Age-related changes in (B) pharyngeal pumping rate and (C) motility in wild-type animals grown on L4440, *F29C4.2(0.2)*, *hsf-1*;L4440(0.2), or *hsf-1;F29C4.2(0.2)* RNAi at 20°C. Values plotted are the mean of at least 20 animals. Error bars denote SEM, and statistical significance was calculated relative to respective L4440 controls by log-rank (Mantel-Cox) test (A) and (two-way ANOVA with Bonferroni correction B and C). $^{**}p < 0.01$; $^{***}p < 0.001$.

Consistent with our RNAi experiments, the enhanced stress resistance conferred by MYb45 or xenobiotics was also almost completely abolished in *hsf-1(sy441)* mutants, suggesting that animals prolong stress resistance in an HSF-1-dependent manner upon encountering mitochondrial-stress-inducing agents (Figures 5E and 5F).

Finally, we examined the relative roles of HSF-1 and ATFS-1 in the ability of mitochondrial perturbation to maintain cytosolic proteostasis with age. Strikingly, we found that *atfs-1(RNAi)* and *skn-1(RNAi)* essentially had no effect on the age-dependent aggregation of intestinal polyQ in the presence of L4440 or *F29C4.2(0.2)(RNAi)* (Figures 5G, 5H, and S5F). In contrast, *hsf-1(RNAi)* accelerated polyQ aggregation in L4440 animals and suppressed the maintenance of proteostasis in *F29C4.2(0.2)(RNAi)* animals by more than 5-fold (Figures 5G and S5F), suggesting that HSF-1 is integral to the ability of reduced ETC function to maintain cytosolic proteostasis and stress resistance.

Mild Mitochondrial Perturbation Increases Longevity and Extends Healthspan in an HSF-1-Dependent Manner

HSF-1 activity is tightly coupled to lifespan, with reduced HSF-1 levels reported to significantly shorten lifespan in wild-type, *daf-2*, *age-1*, and *isp-1;ctb-1* animals (Hsu et al., 2003; Morley and Morimoto, 2004; Walter et al., 2011). However, *hsf-1* has also been shown to be dispensable for lifespan extension conferred by paraquat-induced superoxide and in *isp-1* mutants grown in the presence of fluorodeoxyuridine (FUdR) (Hsu et al., 2003; Yang and Hekimi, 2010).

Given that HSF-1 is crucial for *F29C4.2(0.2)(RNAi)* to maintain proteostasis and stress resistance, we asked whether the ability of mild mitochondrial perturbation to override the repression of the HSR could also improve lifespan and healthspan in an HSF-1-dependent manner. Mild mitochondrial perturbation through *F29C4.2(0.2)(RNAi)* increased both median and maximal lifespan by 50% (Figure 6A). However, increased lifespan through *F29C4.2(0.2)(RNAi)* was not dependent on *atfs-1* (Figure 6A). In addition, *F29C4.2(0.2)(RNAi)* also maintained two well-established markers of healthspan, motility and pharyngeal pumping rate, at a more youthful state into adulthood (Figures 6B and 6C). In contrast, *hsf-1(RNAi)* reduced lifespan and prematurely impaired pharyngeal pumping and paralysis (Figures 6A–6C). Consistent with the dependence on HSF-1 for the maintenance of proteostasis and stress resistance upon ETC perturbation, *hsf-1(RNAi)* significantly truncated lifespan and healthspan to near wild-type levels in *F29C4.2(0.2)(RNAi)* animals (Figures 6A–6C).

Together, our data suggest that signaling through mitochondria can prevent the organismal repression of the HSR in early adulthood in order to preserve proteostasis and maintain somatic health under suboptimal environmental conditions. This has profound effects on lifespan and healthspan and suggests that mitochondria are central regulators of the timing and severity of proteostasis collapse with age.

DISCUSSION

The failure of proteostasis is a central feature of many age-related degenerative disorders, yet little is known regarding the factors that predispose cells to proteostasis collapse with age (Labbadia and Morimoto, 2015b). Here, we report that mitochondrial activity is a key determinant of the long-term activity of the HSR, proteostasis, and healthspan in adulthood and that low levels of mitochondrial stress are sufficient to maintain stress

resistance and cytosolic proteostasis with age in an *hsf*-1-dependent manner.

Reduced mitochondrial activity is associated with increased lifespan in *C. elegans* but typically comes at the cost of reduced fecundity and compromised healthspan (Bansal et al., 2015; Rea et al., 2007; Wang and Hekimi, 2015), suggesting that increased lifespan through ETC perturbation comes at the expense of a poorer quality of life and compromised fitness. Furthermore, genetic interventions that prevent the age-related collapse of proteostasis are associated with reduced brood size or sterility (Shemesh et al., 2013; Labbadia and Morimoto, 2015a), suggesting that the maintenance of proteostasis in adulthood comes at a cost to reproductive capacity. Our studies have revealed that HSF-1 activity, stress resistance, cytosolic proteostasis, and healthspan can all be maintained with age, without causing reduced brood size, through exposure to mild mitochondrial stress.

Our proposal of a relationship between mitochondria and the integrity of the cytosolic proteome is not without precedent, as recent work has demonstrated a complex interplay between mitochondrial function and cytosolic proteostasis in yeast and *C. elegans* (Baker et al., 2012; Kim et al., 2016; Livnat-Levanon et al., 2014; Rainbolt et al., 2013; Ruan et al., 2017; Segref et al., 2014; Wang and Chen, 2015; Wrobel et al., 2015). Given that the vast majority of mitochondrial proteins are nuclear encoded and synthesized in the cytosol, it seems logical for cells to coordinate mitochondrial status with HSF-1 activity and cytosolic proteostasis. However, it had widely been accepted that changes in mitochondrial function do not alter HSF-1 activity, primarily because previous experiments were carried out early in life and/or solely in the context of mitochondrial stress (Yoneda et al., 2004; Kim et al., 2016). Our work challenges this view and suggests that contrary to previous reports, relatively mild ETC disruption does influence the activity of HSF-1 by overriding the programmed repression of the HSR in early adulthood. Crucially, we show that this can provide long-term protection against proteotoxicity arising from the appearance of endogenous metastable proteins or from the presence of chronically expressed disease associated polyQ proteins, suggesting that this pathway allows cells to mount a more effective response to any subsequent cytosolic protein misfolding that might occur as a consequence of age or environmental insults. Furthermore, our work suggests that changes in cytosolic proteostasis arise as a short-term survival adaptation to profound defects in mitochondrial protein import (Wrobel et al., 2015; Wang and Chen, 2015) but can also be triggered by subtle stresses or environmental cues to provide long-term organismal benefits.

Recently, changes in lipid biogenesis as a consequence of *hsp*-6 (mitochondrial HSP70) knockdown were shown to constitutively activate a mitochondrial/cytosolic stress response (McSR) through increased activity of ATFS-1 and HSF-1 (Kim et al., 2016). Our findings are distinct from these observations, as activation of the McSR does not occur from ETC perturbation and results in the constitutive induction of a subset of HSR genes when mitochondria are under severe duress (Kim et al., 2016). Our work suggests that a more nuanced relationship between mitochondrial stress and cytosolic protein quality control exists and that this has a direct impact on the initiation of proteostasis collapse and aging. Furthermore, our work implies that the sensing of protein folding stress can be transmitted across compartments in order to protect against subsequent stresses with age. As such, it will be crucial to understand to what extent, if at all, regulation of the age-related repression of the HSR is reliant on previously described modifiers of mitochondrial retrograde signaling.

An important question that arises from our work is whether maintenance of the HSR through mitochondrial stress is a physiologically relevant phenomenon. Our studies rule out the idea that maintenance of the HSR by mitochondrial perturbation is relevant only under circumstances where organismal health is challenged or crippled by extreme environmental adversity, as stress resistance, proteostasis, and healthspan can be maintained with minimal physiological disruption. Mitochondrial perturbation occurs naturally through imbalances in mitochondrial DNA, exposure to chemicals, and infection by bacterial pathogens (Gitschlag et al., 2016; Lin et al., 2016; Liu et al., 2014; Moullan et al., 2015; Pellegrino et al., 2014). We find that early life exposure to chemicals or microbes that can protract the reproductive period and lead to developmental delay in high doses leads to the maintenance of stress resistance and cytosolic proteostasis in adulthood. This suggests that the ability to sense and adapt to potential threats to fitness before committing to reproduction could allow animals to delay egg-laying until more favorable conditions are found. Therefore, we propose that mitochondria can serve as "sentinels" to gauge fluctuations in the surrounding environment in order to influence the organismal "choice" to commit to programs that initiate reproduction at the cost of the soma, thereby preventing the repression of the HSR until animals find more favorable conditions in which to reproduce.

In summary, our findings provide links among mitochondrial function, regulation of the HSR, and proteostasis that may have important implications in our understanding of how different pathways converge to regulate rates of aging and fecundity. We propose that a greater understanding of the regulatory link between HSF-1 and mitochondrial function will be crucial as we attempt to uncover the drivers of proteostasis collapse in order to promote healthy aging.

EXPERIMENTAL PROCEDURES

Worm Maintenance and Strains

Worms were maintained using standard techniques as previously described (Brenner, 1974). All experiments were conducted at 20°C unless stated otherwise. Strains used in this study were wild-type (N2), Bristol, MQ887 *isp-1(qm150) IV*, MQ1333 *nuo-6(qm200) I*, MQ130 *clk-1(qm30) III*, MQ989 *isp-1(qm150) IV;ctb-1(qm89)*, TK22 *mev-1(kn1)III*, CW152 *gas-1(fc21) X*, NL1832 *ucr-2.3(pk732) III*, AM722 *rmIs288[C12C8.1(hsp-70)p::mCherry; myo-2p::CFP]*, SJ4100 *zcIs13[hsp-6p*::GFP] *V*, EU1 *skn-1(zu67) IV/nT1[unc-?(n754) let-?(IV;V)*, SJ4005 *zcIs4[hsp-4p*::GFP*] V*, CL2166 *dvIs19[gst-4p*::GFP::NLS*] III*, AM738 *rmIs297[vha-6p::Q44::YFP; rol-6(su1006)]*, AM140 *rmIs132[unc-54p::Q35::YFP]*, CB1301 *unc-54(e1301ts) I*, CB1402 *unc-15(e1402ts) I*, AM1061 *unc-119(ed9)III*, *rmSi1[hsf-1p(4kb)::hsf-1(minigene)::gfp::3′UTR(hsf-1) + Cbrunc-119(+)] II; hsf-1(ok600) I*, PS3551 *hsf-1(sy441) I*, and TM4525 *atfs-1(tm4525) V*.

RNAi and Creation of Dilutions

RNAi was essentially performed as previously described (Kamath and Ahringer, 2003), with some modifications. Nematode growth media (NGM) plates

containing 100 μg/mL ampicillin and 1 mM isopropyl β-D-thiogalatoside (IPTG; Sigma) were seeded with RNAi cultures. RNAi bacteria was grown in LB containing 100 μg/mL ampicillin at 37°C for 14 hr and then induced with 5 mM IPTG for a further 3 hr at 37°C with continuous shaking. RNAi dilutions were created by thoroughly mixing RNAi cultures at an optical density 600 (OD_{600}) of 1.5–1.6 with L4440 bacterial cultures at the same OD_{600}. All RNAi clones used in this study were confirmed by sequencing.

Chemical Treatment of Worms and Growth on Alternate Microbes

Antimycin A (sigma) or rotenone (sigma) was dissolved in DMSO and added to NGM plates to the desired concentration before pouring. Plates containing 1% DMSO (v/v) were used as controls. Plates were seeded with OP50 *E. coli* and allowed to dry thoroughly before use. Worms were synchronized to xenobiotic plates by egg-laying and allowed to develop until the late L4 stage before being transferred to control plates for HS at day 2 of adulthood. Chemical containing NGM plates were stored at 4°C until use and always used within 2 weeks of pouring. For culturing worms on *Microbacterium* MYb45, *achromobacter* MYb9, and *stenotrophomonas* MYb57, all bacterial lines were grown and seeded onto standard NGM plates and then allowed to dry for 3 days at room temperature. All microbial plates were used within 1 week of seeding.

RNA Extraction and Real-Time qPCR

RNA extraction and real-time qPCR were performed as previously described (Labbadia and Morimoto, 2015a). Briefly, worms were lysed in 250 μL TRIzol (Invitrogen), vigorously shaken with chloroform, allowed to stand for 3 min at room temperature, and then centrifuged at 16,000 × *g* at 4°C. The aqueous phase was then collected, and RNA was purified using QIAGEN RNeasy min-elute columns and genomic DNA (gDNA) eliminator columns as per the manufacturer's instructions. cDNA was synthesized from 500 ng RNA using an iScript cDNA synthesis kit (Bio-Rad). Real-time qPCR reactions were performed in triplicate for each gene using iQ SYBR green super mix (Bio-Rad) using a Bio-Rad iCycler iQ real-time PCR detection system. Relative expression of genes was determined using the relative standard curve method. All primers used can be found in Table S1.

Thermorecovery Assays

Thermorecovery assays were performed as previously described (Labbadia and Morimoto, 2015a), with the exception that lethal HS was measured as relative motility or survival following either a non-lethal HS (33°C, 6 hr) or a lethal HS (35°C, 4 hr), respectively. For non-lethal thermorecovery, 25–30 animals were picked onto new seeded plates, wrapped tightly with parafilm, and submerged in a water bath at 33°C for 6 hr. Following HS treatment, worms were allowed to recover for 48 hr at 20°C, after which, the proportion of the population moving normally in response to 3 plate taps was scored. Animals were scored as having abnormal movement if they exhibited paralysis, uncoordinated sinusoidal movement, sluggishness/lethargy (moving less than 1 body length per second), or irresponsiveness to plate tap. Lethal HS was conducted in the same manner but in a water bath at 35°C for 4 hr. Survival was then scored at 24-hr intervals following HS until the entire population was dead. Worms were scored as dead in the complete absence of touch response and pharyngeal pumping.

Fecundity Assays

Worms were singled onto 3-cm plates seeded with bacteria on the first day of adulthood and allowed to lay eggs. Worms were then transferred to new plates every day throughout adulthood until egg-laying had ceased, and plates containing eggs were incubated at 20°C for 48 hr, after which the number of progeny produced on each day of adulthood was counted. The mean number of progeny produced on each day of adulthood was calculated from 20 worms per treatment group.

Motility Assays

Assessment of animal motility with age was conducted as previously described (Nussbaum-Krammer et al., 2015). Briefly, 30–40 age-synchronized worms were picked onto NGM plates with a thin bacterial lawn and allowed to acclimatize for 30 min. Worms were transferred to new plates to remove progeny. Plates were tapped 3 times to stimulate movement and motility was then recorded for 30 s. Motility videos were captured using a Leica stereomicroscope at 10× magnification with a Hamamatsu Orca-R2 digital camera C10600-10B and Hamamatsu Simple PCI imaging software.

Pharyngeal Pumping Assays

To score pumping rates with age, worms were transferred individually to new plates, and pharyngeal pumping was counted for 6 independent periods of 10 s to obtain the number of contractions per minute. Pumping was scored for 20 worms per group, and the average number of contractions per minute was then calculated for each population of worms.

Lifespan Assays

Worms were allowed to reach adulthood and then scored for dead worms every other day throughout life. Animals were transferred to new plates every day for the first 7 days of adulthood and then transferred to new plates every 4 days thereafter. Worms were scored as dead in the absence of pharyngeal pumping and response to touch with a platinum pick.

Fluorescence Microscopy

Worms were imaged by mounting on 5% agarose pads in 3 mM levamisole. Fluorescence and bright-field images of reporter worms were acquired using a Zeiss Axiovert 200 microscope, a Hamamatsu Orca 100 cooled CCD camera, and Zeiss Axiovision software. Images of intestinal and body wall muscle polyQ aggregates were captured using a Leica SP5 II laser scanning confocal microscope equipped with HyD detectors. Acquisition parameters were kept identical across samples.

Statistical Analyses

Statistical significance was calculated using the log-rank (Mantel-Cox) test for lifespan assays. Either one-way ANOVA with Tukey post analysis pairwise comparison of groups, two-way ANOVA with Bonferroni post-analysis correction, or two-tailed Student's t test were used for all other comparisons as stated in figure legends. The statistical tests used are declared in all figure legends and were calculated using GraphPad Prism (ANOVA and log-rank) or Microsoft Excel (Student's t test).

SUPPLEMENTAL INFORMATION

Supplemental Information includes Supplemental Experimental Procedures, five figures, and two tables and can be found with this article online at https://doi.org/10.1016/j.celrep.2017.10.038.

AUTHOR CONTRIBUTIONS

J.L. designed and performed experiments, analyzed data, and constructed figures. R.I.M. designed experiments and analyzed data. J.L., R.M.B., and M.F.N. performed genome-wide RNAi screening. Y.-F.L. and C.M.H. designed and performed oxygen consumption experiments. J.L. and R.I.M. wrote the manuscript with input from Y.-F.L., C.M.H., R.M.B., and M.F.N.

ACKNOWLEDGMENTS

We thank Ilya Ruvinsky, Yoko Shibata, and Jian Li for critical reading of the manuscript and the Keck Biophysics, High Throughput Analysis, and Biological Imaging Facilities at Northwestern University for equipment use. The anti-HSP-16 antibody was a kind gift from Gordon Lithgow, and the anti-HSP-6 antibody was generated by Cindy Voisine. MYb bacterial strains were a kind gift from Hinrich Schulenburg. We also thank David Gems for the use of general equipment and reagents. Many of the strains used in this study were provided by the CGC, which is funded by the NIH Office of Research Infrastructure Programs (grant P40 OD010440). Strain TM4525 was provided by the National Bioresource Project (Tokyo, Japan). This work was supported by NIH (National Institute on Aging) grant R01AG026647, the Ellison Medical Foundation, and the Daniel F. and Ada L. Rice Foundation (to R.I.M.) and grant R01AG047182 (to C.M.H.), as well as an ALS Association Milton Safenowitz postdoctoral fellowship and a BBSRC David Phillips fellowship (BB/P005535/1) to J.L..

Received: April 9, 2017
Revised: September 18, 2017
Accepted: October 10, 2017
Published: November 7, 2017

REFERENCES

Akerfelt, M., Morimoto, R.I., and Sistonen, L. (2010). Heat shock factors: integrators of cell stress, development and lifespan. Nat. Rev. Mol. Cell Biol. *11*, 545–555.

Baker, B.M., Nargund, A.M., Sun, T., and Haynes, C.M. (2012). Protective coupling of mitochondrial function and protein synthesis via the eIF2α kinase GCN-2. PLoS Genet. *8*, e1002760.

Bansal, A., Zhu, L.J., Yen, K., and Tissenbaum, H.A. (2015). Uncoupling lifespan and healthspan in Caenorhabditis elegans longevity mutants. Proc. Natl. Acad. Sci. USA *112*, E277–E286.

Baruah, A., Chang, H., Hall, M., Yuan, J., Gordon, S., Johnson, E., Shtessel, L.L., Yee, C., Hekimi, S., Derry, W.B., and Lee, S.S. (2014). CEP-1, the Caenorhabditis elegans p53 homolog, mediates opposing longevity outcomes in mitochondrial electron transport chain mutants. PLoS Genet. *10*, e1004097.

Ben-Zvi, A., Miller, E.A., and Morimoto, R.I. (2009). Collapse of proteostasis represents an early molecular event in Caenorhabditis elegans aging. Proc. Natl. Acad. Sci. USA *106*, 14914–14919.

Bennett, C.F., Vander Wende, H., Simko, M., Klum, S., Barfield, S., Choi, H., Pineda, V.V., and Kaeberlein, M. (2014). Activation of the mitochondrial unfolded protein response does not predict longevity in Caenorhabditis elegans. Nat. Commun. *5*, 3483.

Brenner, S. (1974). The genetics of Caenorhabditis elegans. Genetics *77*, 71–94.

Butler, J.A., Ventura, N., Johnson, T.E., and Rea, S.L. (2010). Long-lived mitochondrial (Mit) mutants of Caenorhabditis elegans utilize a novel metabolism. Faseb. J. *24*, 4977–4988.

David, D.C., Ollikainen, N., Trinidad, J.C., Cary, M.P., Burlingame, A.L., and Kenyon, C. (2010). Widespread protein aggregation as an inherent part of aging in C. elegans. PLoS Biol. *8*, e1000450.

Dillin, A., Hsu, A.L., Arantes-Oliveira, N., Lehrer-Graiwer, J., Hsin, H., Fraser, A.G., Kamath, R.S., Ahringer, J., and Kenyon, C. (2002). Rates of behavior and aging specified by mitochondrial function during development. Science *298*, 2398–2401.

Dirksen P, Marsh SA, Braker I, Heitland N, Wagner S, Nakad R, Mader S, Petersen C, Kowallik V, Rosenstiel P, Félix MA, and Schulenburg H. (2016). The native microbiome of the nematode Caenorhabditis elegans: gateway to a new host-microbiome model. BMC Biol. *9*;14:38.

Durieux, J., Wolff, S., and Dillin, A. (2011). The cell non-autonomous nature of electron transport chain-mediated longevity. Cell *144*, 79–91.

Feng, J., Bussière, F., and Hekimi, S. (2001). Mitochondrial electron transport is a key determinant of life span in Caenorhabditis elegans. Dev. Cell *1*, 633–644.

Gitschlag, B.L., Kirby, C.S., Samuels, D.C., Gangula, R.D., Mallal, S.A., and Patel, M.R. (2016). Homeostatic Responses Regulate Selfish Mitochondrial Genome Dynamics in C. elegans. Cell Metab. *24*, 91–103.

Haynes, C.M., Yang, Y., Blais, S.P., Neubert, T.A., and Ron, D. (2010). The matrix peptide exporter HAF-1 signals a mitochondrial UPR by activating the transcription factor ZC376.7 in C. elegans. Mol. Cell *37*, 529–540.

Houtkooper, R.H., Mouchiroud, L., Ryu, D., Moullan, N., Katsyuba, E., Knott, G., Williams, R.W., and Auwerx, J. (2013). Mitonuclear protein imbalance as a conserved longevity mechanism. Nature *497*, 451–457.

Hsu, A.L., Murphy, C.T., and Kenyon, C. (2003). Regulation of aging and age-related disease by DAF-16 and heat-shock factor. Science *300*, 1142–1145.

Kamath, R.S., and Ahringer, J. (2003). Genome-wide RNAi screening in Caenorhabditis elegans. Methods *30*, 313–321.

Kim, Y., and Sun, H. (2007). Functional genomic approach to identify novel genes involved in the regulation of oxidative stress resistance and animal lifespan. Aging Cell *6*, 489–503.

Kim, H.E., Grant, A.R., Simic, M.S., Kohnz, R.A., Nomura, D.K., Durieux, J., Riera, C.E., Sanchez, M., Kapernick, E., Wolff, S., et al. (2016). Lipid biosynthesis coordinates a mitochondrial-to-cytosolic stress response. Cell *166*, 1539–1552.

Labbadia, J., and Morimoto, R.I. (2014). Proteostasis and longevity: when does aging really begin? F1000Prime Rep. *6*, 7.

Labbadia, J., and Morimoto, R.I. (2015a). Repression of the heat shock response is a programmed event at the onset of reproduction. Mol. Cell *59*, 639–650.

Labbadia, J., and Morimoto, R.I. (2015b). The biology of proteostasis in aging and disease. Annu. Rev. Biochem. *84*, 435–464.

Lakowski, B., and Hekimi, S. (1996). Determination of life-span in Caenorhabditis elegans by four clock genes. Science *272*, 1010–1013.

Lee, S.S., Lee, R.Y., Fraser, A.G., Kamath, R.S., Ahringer, J., and Ruvkun, G. (2003). A systematic RNAi screen identifies a critical role for mitochondria in C. elegans longevity. Nat. Genet. *33*, 40–48.

Li, J., Chauve, L., Phelps, G., Brielmann, R.M., and Morimoto, R.I. (2016). E2F coregulates an essential HSF developmental program that is distinct from the heat-shock response. Genes Dev. *30*, 2062–2075.

Li, J., Labbadia, J., and Morimoto, R.I. (2017). Rethinking HSF1 in stress, development, and organismal health. Trends Cell Biol. *17*, 30139–30150.

Lin, Y.F., Schulz, A.M., Pellegrino, M.W., Lu, Y., Shaham, S., and Haynes, C.M. (2016). Maintenance and propagation of a deleterious mitochondrial genome by the mitochondrial unfolded protein response. Nature *533*, 416–419.

Liu, Y., Samuel, B.S., Breen, P.C., and Ruvkun, G. (2014). Caenorhabditis elegans pathways that surveil and defend mitochondria. Nature *508*, 406–410.

Livnat-Levanon, N., Kevei, É., Kleifeld, O., Krutauz, D., Segref, A., Rinaldi, T., Erpapazoglou, Z., Cohen, M., Reis, N., Hoppe, T., and Glickman, M.H. (2014). Reversible 26S proteasome disassembly upon mitochondrial stress. Cell Rep. *7*, 1371–1380.

López-Otín, C., Blasco, M.A., Partridge, L., Serrano, M., and Kroemer, G. (2013). The hallmarks of aging. Cell *153*, 1194–1217.

Mohri-Shiomi, A., and Garsin, D.A. (2008). Insulin signaling and the heat shock response modulate protein homeostasis in the Caenorhabditis elegans intestine during infection. J. Biol. Chem. *283*, 194–201.

Morley, J.F., and Morimoto, R.I. (2004). Regulation of longevity in Caenorhabditis elegans by heat shock factor and molecular chaperones. Mol. Biol. Cell *15*, 657–664.

Moullan, N., Mouchiroud, L., Wang, X., Ryu, D., Williams, E.G., Mottis, A., Jovaisaite, V., Frochaux, M.V., Quiros, P.M., Deplancke, B., et al. (2015). Tetracyclines disturb mitochondrial function across eukaryotic models: a call for caution in biomedical research. Cell Rep. Published online March 10, 2015. https://doi.org/10.1016/j.celrep.2015.02.034.

Nargund, A.M., Fiorese, C.J., Pellegrino, M.W., Deng, P., and Haynes, C.M. (2015). Mitochondrial and nuclear accumulation of the transcription factor ATFS-1 promotes OXPHOS recovery during the UPR(mt). Mol. Cell *58*, 123–133.

Nussbaum-Krammer, C.I., Neto, M.F., Brielmann, R.M., Pedersen, J.S., and Morimoto, R.I. (2015). Investigating the spreading and toxicity of prion-like proteins using the metazoan model organism C. elegans. J. Vis. Exp. *95*, 52321.

Pellegrino, M.W., Nargund, A.M., Kirienko, N.V., Gillis, R., Fiorese, C.J., and Haynes, C.M. (2014). Mitochondrial UPR-regulated innate immunity provides resistance to pathogen infection. Nature *516*, 414–417.

Prahlad, V., and Morimoto, R.I. (2011). Neuronal circuitry regulates the response of Caenorhabditis elegans to misfolded proteins. Proc. Natl. Acad. Sci. USA *108*, 14204–14209.

Rainbolt, T.K., Atanassova, N., Genereux, J.C., and Wiseman, R.L. (2013). Stress-regulated translational attenuation adapts mitochondrial protein import through Tim17A degradation. Cell Metab. *18*, 908–919.

Rea, S.L., Ventura, N., and Johnson, T.E. (2007). Relationship between mitochondrial electron transport chain dysfunction, development, and life extension in Caenorhabditis elegans. PLoS Biol. *5*, e259.

Reis-Rodrigues, P., Czerwieniec, G., Peters, T.W., Evani, U.S., Alavez, S., Gaman, E.A., Vantipalli, M., Mooney, S.D., Gibson, B.W., Lithgow, G.J., and Hughes, R.E. (2012). Proteomic analysis of age-dependent changes in protein solubility identifies genes that modulate lifespan. Aging Cell *11*, 120–127.

Ruan, L., Zhou, C., Jin, E., Kucharavy, A., Zhang, Y., Wen, Z., Florens, L., and Li, R. (2017). Cytosolic proteostasis through importing of misfolded proteins into mitochondria. Nature *543*, 443–446.

Samuel, B.S., Rowedder, H., Braendle, C., Félix, M.A., and Ruvkun, G. (2016). Caenorhabditis elegans responses to bacteria from its natural habitats. Proc. Natl. Acad. Sci. USA *113*, E3941–E3949.

Schaar, C.E., Dues, D.J., Spielbauer, K.K., Machiela, E., Cooper, J.F., Senchuk, M., Hekimi, S., and Van Raamsdonk, J.M. (2015). Mitochondrial and cytoplasmic ROS have opposing effects on lifespan. PLoS Genet. *11*, e1004972.

Segref, A., Kevei, É., Pokrzywa, W., Schmeisser, K., Mansfeld, J., Livnat-Levanon, N., Ensenauer, R., Glickman, M.H., Ristow, M., and Hoppe, T. (2014). Pathogenesis of human mitochondrial diseases is modulated by reduced activity of the ubiquitin/proteasome system. Cell Metab. *19*, 642–652.

Shemesh, N., Shai, N., and Ben-Zvi, A. (2013). Germline stem cell arrest inhibits the collapse of somatic proteostasis early in Caenorhabditis elegans adulthood. Aging Cell *12*, 814–822.

Taylor, R.C., and Dillin, A. (2013). XBP-1 is a cell-nonautonomous regulator of stress resistance and longevity. Cell *153*, 1435–1447.

Walter, L., Baruah, A., Chang, H.W., Pace, H.M., and Lee, S.S. (2011). The homeobox protein CEH-23 mediates prolonged longevity in response to impaired mitochondrial electron transport chain in C. elegans. PLoS Biol. *9*, e1001084.

Walther, D.M., Kasturi, P., Zheng, M., Pinkert, S., Vecchi, G., Ciryam, P., Morimoto, R.I., Dobson, C.M., Vendruscolo, M., Mann, M., and Hartl, F.U. (2015). Widespread proteome remodeling and aggregation in aging C. elegans. Cell *161*, 919–932.

Wang, X., and Chen, X.J. (2015). A cytosolic network suppressing mitochondria-mediated proteostatic stress and cell death. Nature *524*, 481–484.

Wang, Y., and Hekimi, S. (2015). Mitochondrial dysfunction and longevity in animals: untangling the knot. Science *350*, 1204–1207.

Wrobel, L., Topf, U., Bragoszewski, P., Wiese, S., Sztolsztener, M.E., Oeljeklaus, S., Varabyova, A., Lirski, M., Chroscicki, P., Mroczek, S., et al. (2015). Mistargeted mitochondrial proteins activate a proteostatic response in the cytosol. Nature *524*, 485–488.

Yang, W., and Hekimi, S. (2010). A mitochondrial superoxide signal triggers increased longevity in Caenorhabditis elegans. PLoS Biol. *8*, e1000556.

Yoneda, T., Benedetti, C., Urano, F., Clark, S.G., Harding, H.P., and Ron, D. (2004). Compartment-specific perturbation of protein handling activates genes encoding mitochondrial chaperones. J. Cell Sci. *117*, 4055–4066.

Yun, J., and Finkel, T. (2014). Mitohormesis. Cell Metab. *19*, 757–766.

Cell Reports, Volume *21*

Supplemental Information

Mitochondrial Stress Restores the Heat Shock Response and Prevents Proteostasis Collapse during Aging

Johnathan Labbadia, Renee M. Brielmann, Mario F. Neto, Yi-Fan Lin, Cole M. Haynes, and Richard I. Morimoto

Supplemental information

Supplemental experimental procedures

Supplemental figures 1 – 5

Supplemental figure legends

Supplemental tables S1 and S2

Supplemental experimental procedures

Chromatin immunoprecipitation

Chromatin immunoprecipitation was essentially performed as previously described (Labbadia and Morimoto, 2015a). Approximately 10,000 bleach synchronized L1 larvae were grown on 10 cm RNAi plates seeded with RNAi bacteria (approx. 500 worms per plate). Animals were subjected to control or heat shock (33°C, 30 minutes) conditions at day 2 of adulthood by submerging parafilmed plates in a large water bath. Day 2 adults were then washed off large plates in M9 and allowed to gravity sediment for 1 -2 minutes. Eggs and L1 larvae suspended in the "supernatant" were removed and the process was repeated 3 times to ensure the removal of all progeny (confirmed by examining 20 µl aliquots of packed adult worms on a glass slide under a light microscope). Chromatin cross-linking was performed by gently agitating worms in 1% formaldehyde in PBS on a nutator at room temperature for 30 min with intermittent douncing of worms to promote disruption of the cuticle. Cross-linking was quenched by incubation with 125 mM glycine for 10 minutes at room temperature. Worms were then pelleted and washed 3 times with ice-cold FA buffer (50 mM HEPES/KOH pH7.5, 1 mM EDTA, 1% Triton X-100, 0.1% sodium deoxyholate, 150 mM NaCl with Roche Complete protease inhibitors). Worm pellets were then re-suspended in 500 µl of FA buffer and dounce homogenized on ice for 30 – 60 minutes to completely break-up worms. Animals were further broken up by sonication on high power (30s on, 60s off) using a Bioruptor sonicator (Diagenode). Complete destruction of worms was confirmed by examination of 2 µl of worm chromatin samples under a light microscope and chromatin preps were then centrifuged at 17,000*g* for 15 min at 4°C. Chromatin was sheared to 200 - 500 base pair fragments with an additional 2 rounds of sonication on high power (30s on, 60s off) and shearing efficiency was examined by electrophoresis of 5 µl of reverse cross-linked chromatin on a 1% agarose gel. Pulldowns were set up using 2 mg of protein, 20 µl of protein-G dynabeads (Invitrogen), and either 5 µl of anti-full length GFP antibody (Clontech, living colors), or 2 µg of anti-AMA-1 antibody (Novus Biological) in FA buffer (1 ml total volume). Pulldowns were then incubated at 4°C overnight on a rotator. Following incubation, protein-G dynabeads were washed were washed at room temperature 2 times for 5 minutes in FA buffer, then once for 10 minutes in FA buffer with 500mM NaCl, once for 5 minutes in FA buffer with 1M NaCl, once in for 10 minutes in TEL buffer (0.25M LiCl, 1% NP-40, 1% sodium deoxyholate, 1mM EDTA, 10mM Tris-HCl, pH 8.0), and twice for 5 minutes in TE pH 8.0. DNA was eluted twice by incubating beads with 50 µl elution buffer (TE containing 1% SDS and 250mM NaCl) at 65°C for 30 minutes each time. 10% of input

DNA was also diluted in 100 µl elution buffer and processed in parallel with ChIP samples. Eluted DNA was treated with RNase A for 30 minutes at 37°C and then with 0.1 mg/ml Proteinase K for 1 hour at 50°C. Crosslinking was then reversed at 65°C overnight and DNA samples were purified using Qiagen PCR purification columns. Levels of ChIP DNA relative to inputs were then determined by RT-qPCR using the relative standard curve method of quantification. Primers used can be found in Table S2.

Western blotting

Briefly, 50 – 100 day 2 adult animals were picked directly into 20 µl of Laemmli loading buffer and incubated at 95°C for 5 minutes. 5 µl of sample was then separated by SDS-PAGE and transferred to a nitrocellulose membrane. Blots were then blocked for 1 hour at room temperature with 5% non-fat milk in PBS (w/v) and washed 3 times in PBS 0.2% Tween (v/v). Blots were then incubated with primary antibodies for 1 hour at room temperature in PBS 0.02% Tween (anti-tubulin 1:10,000, anti-HSP-6 1:1000) or over-night at 4°C in 0.5% non-fat milk in PBS with 0.02% Tween (anti-GFP 1:1000, anti-HSP-16 1:1000) and then washed three times for 10 minutes with PBS-0.2% Tween. Membranes were then incubated for 1 hour at room temperature with HRP conjugated secondary antibodies in PBS 0.02% Tween, washed three times for 15 minutes in PBS-0.2% Tween, and then exposed to ECL Plus (Amersham) as per manufacturer's instructions to develop signal. Blots were imaged using a PXi multi-application gel imaging system (Syngene) and the densitometry of bands was quantified using image J. The anti HSP-6 antibody was generated by Thermo Scientific Open Biosystems by immunizing rabbits against a DAQEAKTAEEPKKEQN peptide corresponding to amino acids 642 - 657of the C-terminus of *C. elegans* HSP-6 (C37H5.8).

Genome-wide RNAi screening

Genome-wide screening was essentially conducted as previously described (Silva et al., 2011) using an RNAi library constructed by the Ahringer laboratory (Kamath et al., 2003) and consisting of bacteria expressing dsRNA against approximately 87% of predicted *C. elegans* genes. RNAi bacterial cultures were grown at 37°C with continuous shaking (315 rpm, Orbital shaker, GeneMachines HiGro, Genomic Solutions, USA) in 96 well plate format for 14 hours in 65 µl LB containing 50 µg/ml ampicillin. Bacterial cultures were then induced for 3 hours at 37°C with 0.5 mM of isopropyl β-D-thiogalatoside (IPTG, Sigma). Approximately 15 – 20 bleach synchronized wild type (N2)

L1 larvae were added to each well of a 96-well plate in 50 µl of M9 containing 1 µg/ml cholesterol, 50 µg/ml ampicillin, 10 µg/ml tetracycline, 0.1 µg/ml fungizone and 170 µg/ml IPTG and incubated at 20°C with continuous shaking (200 rpm, Innova 4430 Incubator Shaker, New Brunswick, USA). At day 2 of adulthood (70-74h post plating L1s) 96-well RNAi plates containing worms were placed in an incubator at 35°C in pre-warmed perspex boxes (approximately 6 plates per box) and heat shocked for 5 hours. Plates were then placed back at 20°C with continuous shaking and the population of each well was scored for motility (i.e. the proportion of worms exhibiting any form of thrashing regardless of speed) 24 hours later. RNAi clones were scored as hits in the preliminary round if ≥ 30% of animals were moving. Preliminary hits (93 genes) were then re-arrayed on new 96-well plates and subjected to validation screening in liquid to remove false positives. Following this, final clones (51 genes) were screened three times on solid media and clones that restored movement to ≥ 50% of the population in all 3 trials were taken as final hits.

Oxygen Consumption and ATP measurements

Oxygen consumption was measured using a Seahorse XF^{e}96 Analyzer at 25°C similar to that described previously (Andreux et al., 2014). In brief, worms raised on vector or RNAi bacteria were transferred onto empty plates at indicated stages and allowed to completely digest the remaining bacteria for 1 hour, after which 4 worms were transferred into each well of a 96-well microplate containing 200 µl M9 buffer. Basal respiration was measured for a total of 60 minutes, in 6 minute intervals that included a 2 minute mix, a 2 minute time delay and a 2 minute measurement. ATP levels were quantified using a luciferase based ATP detection kit (Thermo) as per manufacturer's instructions. Briefly, 10 µl of RIPA buffer lysate from 200 worms was incubated with luciferin and luciferase in ATP detection buffer without ATP. Luminescence was then measured using a Tecan M200 microplate reader and levels of ATP were calculated from a series of ATP standards of known concentration.

ROS measurements

ROS levels were quantified in whole worms using the fluorescent substrate DHE (Thermo) (various forms of ROS), the Amplex-Red H_2O_2 detection kit (Thermo) (for hydrogen peroxide), or the Oxyblot detection system (Millipore) (for total carbonylated protein). DHE fluorescence was measured by placing 100 worms in M9 containing 4 µM DHE

(after washing twice in M9 to remove bacteria) and incubating in the dark with gentle agitation for 30 min at room temperature. Worms were then washed 3 times in M9 and placed in each well of a Costar 96-well, black, polystyrene plate (in 100 µl M9). The fluorescence intensity of each well was then measured (Ex/Em 358/461 non-oxidized; 518/606 oxidized) using a Tecan M200 plate reader. Background fluorescence (wells containing worms not treated with DHE) was subtracted from readings and the ratio of oxidized versus non-oxidized DHE was calculated for each treatment group. For H_2O_2 measurements, readings were collected as per manufacturer's instructions. Briefly, 50 µl of fresh lysate from 100 worms (in RIPA buffer) was added to 50 µl of Amplex-Red H_2O_2 detection reagent and incubated in the dark with gentle agitation for 30 min. Fluorescence intensity was then measured (Ex/Em 571/585) using a Tecan M200 plate reader. Background values were subtracted from readings and the amount of H_2O_2 present in each sample was calculated from a standard curve constructed from samples containing known quantities of H_2O_2. Levels of H_2O_2 were then normalized against total protein present in each sample, as determined by BCA assay (Pierce). Levels of carbonylated protein were measured using the Oxyblot system according to manufacturer's instructions. Briefly, 200 worms were lysed in RIPA buffer containing 50 mM DTT to prevent protein oxidation following lysis. 20 µl of each lysate was then incubated with 2,4-dinitrophenylhydrazine (DNPH) for 20 min at room temperature and separated by SDS-PAGE. Following western blotting, membranes were blocked with 5% milk-PBS and incubated for 1 hour at room temperature with rabbit anti-DNP primary antibody (1:150) in 0.02% PBS-Tween. Membranes were then washed three times with 0.2% PBS-Tween and incubated for 1 hour at room temperature with HRP conjugated goat anti-rabbit secondary antibody (1:300) in 0.02% PBS-Tween. Blots were then washed a further three times with 0.2% PBS-Tween and carbonylated proteins were detected using ECL reagent and an LAS4000 ImageQuant detection system (GE). Blots were stripped and re-probed for tubulin as a loading control (mouse anti-tubulin primary (Sigma, 1:5000)). Contrast and brightness were adjusted linearly across entire blots to enhance visibility of detected bands.

Supplemental Figure S1

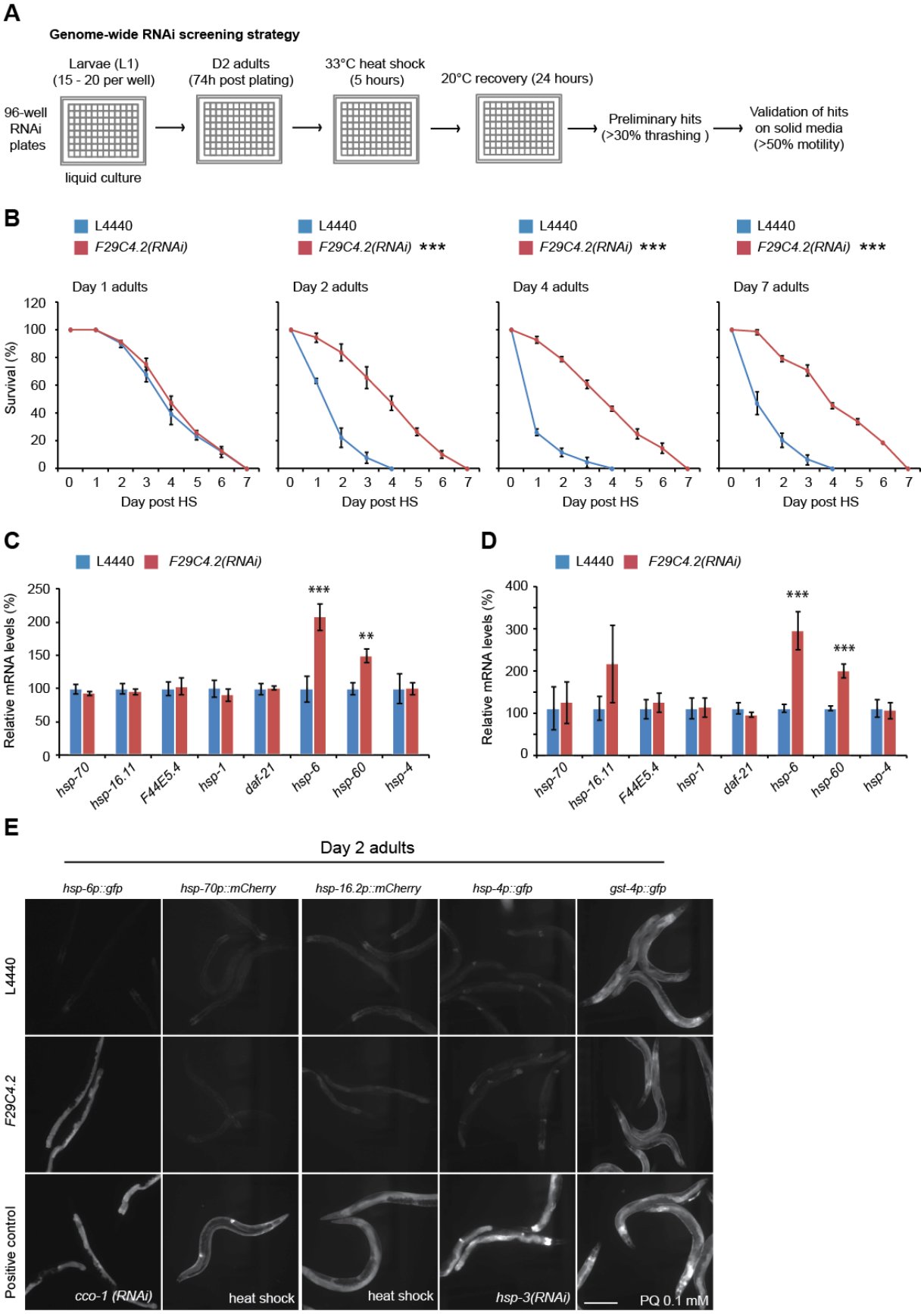

Supplemental figure 1, related to main figure 1. Knockdown of *F29C4.2* constitutively activates the UPR^{mt} but not the UPR^{ER}, HSR or oxidative stress response

(A) Schematic of genome-wide RNAi screening strategy to identify suppressors of stress resistance in reproductively active adults.

(B) Survival of animals following a 4 hour, 35°C heat shock at day 1, 2, 4, or 7 of adulthood following growth on empty vector control (L4440) or *F29C4.2(RNAi)*. Values are the mean of 4 biological replicates and error bars denote SEM. *** = $p < 0.001$. Statistical significance was calculated by two-way ANOVA with Bonferroni correction.

(C and D) Basal expression of *hsp-70(C12C8.1), hsp-16.11, F44E5.4, hsp-1, daf-21, hsp-6, hsp-60,* and *hsp-4* normalized to the housekeeping genes *rpb-2* and *cdc-42* at (C) day 1 or (D) day 2 of adulthood following growth on L4440 or *F29C4.2(RNAi)*. Values are the mean of 4 biological replicates and error bars denote SEM. ** = $p < 0.01$, *** = $p < 0.001$. Statistical significance was calculated by ANOVA with Bonferroni correction.

(E) GFP or mCherry fluorescence at day 2 of adulthood in UPR^{mt} (*hsp-6p::gfp*), UPR^{ER} (*hsp-4p::gfp*), oxidative stress response (*gst-4p::gfp*) and HSR (*hsp-70p::mcherry* and *hsp-16.2p::mcherry*) reporter lines grown on L4440 or *F29C4.2(RNAi)*. Scale bar = 250 µM.

Supplemental Figure 2

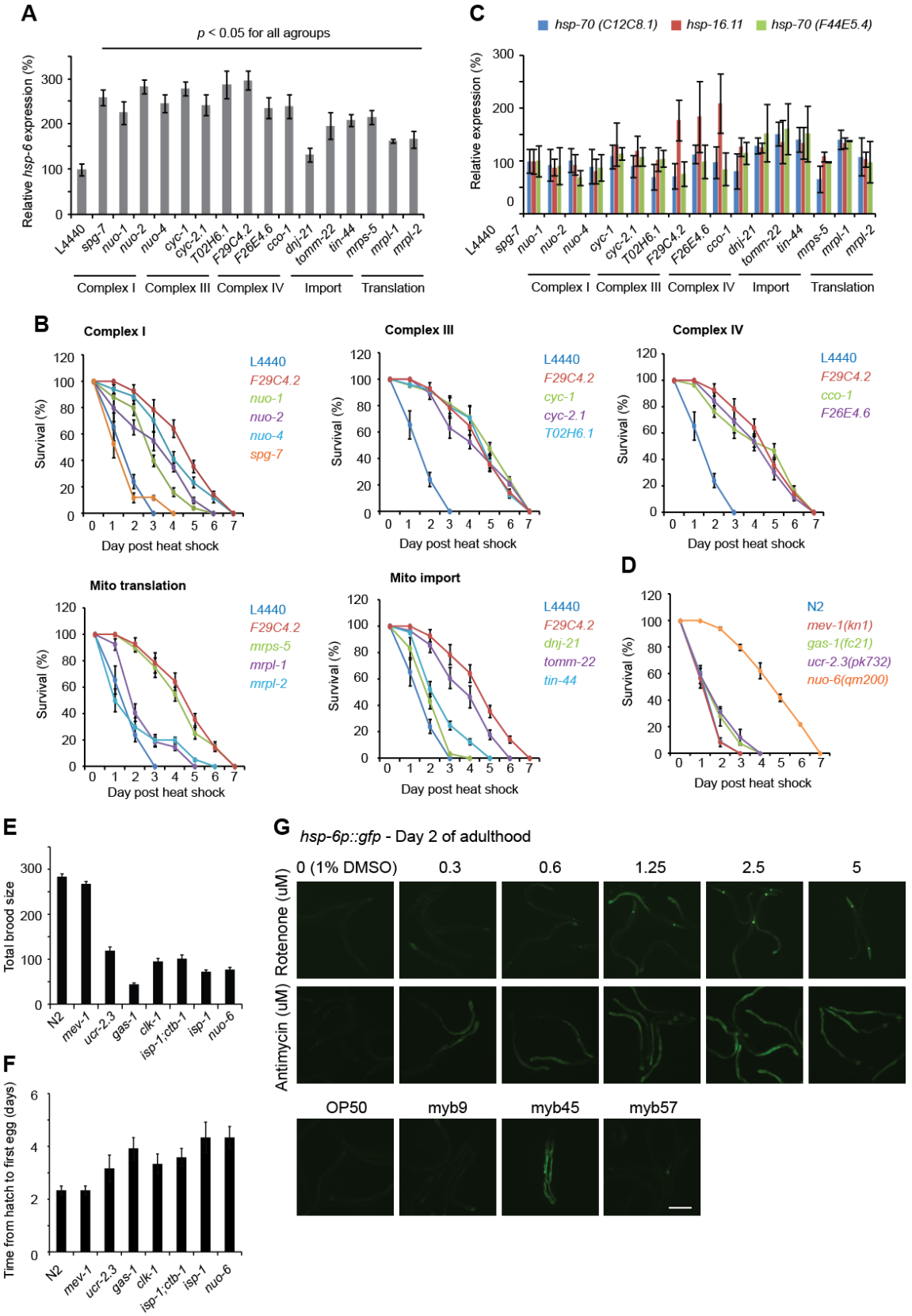

Supplemental Figure 2, related to main figure 2. Mitochondrial perturbation activates the UPR^{mt} but not the HSR

(A) Basal expression of *hsp-6* at day 2 of adulthood in animals grown on empty vector control (L4440) or RNAi against a mitochondrial AAA metalloprotease (*spg*-7), subunits of complex I (*nuo-1, nuo-2, and nuo-4*), complex III (*cyc-1, cyc-2.1, and T02H6.11*), and complex IV (*F29C4.2, F26E4.6, and cco-1*), or components of protein import (*dnj-21, tomm-22, and tin-44*), or mitochondrial translation (*mrps-5, mrpl-1, and mrpl-2*). Expression was calculated relative to the house keeping genes *rpb-2* and *cdc-42.* Values plotted are the mean of 4 biological replicates and bars represent SEM. *P* values were calculated by one-way ANOVA with tukey post analysis pairwise comparison of groups.

(B) Survival following heat shock at 35°C for 4 hours on day 2 of adulthood in wild type (N2) animals grown on L4440 or RNAi against a mitochondrial AAA metalloprotease (*spg*-7), subunits of complex I (*nuo-1, nuo-2, and nuo-4*), complex III (*cyc-1, cyc-2.1, and T02H6.11*), and complex IV (*F29C4.2, F26E4.6, and cco-1*), protein import (*dnj-21, tomm-22, and tin-44*), or mitochondrial translation (*mrps-5, mrpl-1, and mrpl-2*). Values are plotted as mean survival at different days following HS. Error bars represent SEM. L4440 and *F29C4.2* curves are present on all graphs for reference.

(C) *hsp-70(C12C8.1), hsp-70(F44E5.4),* and *hsp-16.11* at day 2 of adulthood in animals grown on empty vector control (L4440) or RNAi against a mitochondrial AAA metalloprotease (*spg*-7), subunits of complex I (*nuo-1, nuo-2, and nuo-4*), complex III (*cyc-1, cyc-2.1, and T02H6.11*), and complex IV (*F29C4.2, F26E4.6, and cco-1*), or components of protein import (*dnj-21, tomm-22, and tin-44*), or mitochondrial translation (*mrps-5, mrpl-1, and mrpl-2*). Expression was calculated relative to the house keeping genes *rpb-2* and *cdc-42.* Values plotted are the mean of 4 biological replicates and bars represent SEM.

(D) Survival following heat shock at 35°C for 4 hours on day 2 of adulthood in wild type (N2), *mev-1(kn1), ucr-2.3(pk732), gas-1(fc21),* and *nuo-6(qm200)* mitochondrial mutants. Values are the mean of 4 biological replicates plotted as mean survival at different days following HS. Error bars represent SEM.

(E) Total brood sizes of wild type (N2) and mitochondrial mutant worms.

(F) Number of days required post hatching for wild type or mitochondrial mutant worms to lay first eggs. In most cases this reflected delayed developmental rates, however, in the case of *ucr-2.3(pk732)* mutants, the delayed time to egg-lay reflected normal developmental timing to adulthood but a delayed appearance of embryos in the gonad.

(**G**) GFP fluorescence at day 2 of adulthood in *hsp-6p::gfp* UPR^{mt} reporter worms following growth on plates containing 0, 0.3, 0.6, 1.25, 2.5, and 5 uM rotenone or antimycin, or plates seeded with OP50 (*E. coli*), MYb9 (*achromobacter*), MYb45 (*microbacterium*), or MYb57 (*stenotrophomonas*). Scale bar = 250 µM.

Supplemental Figure 3

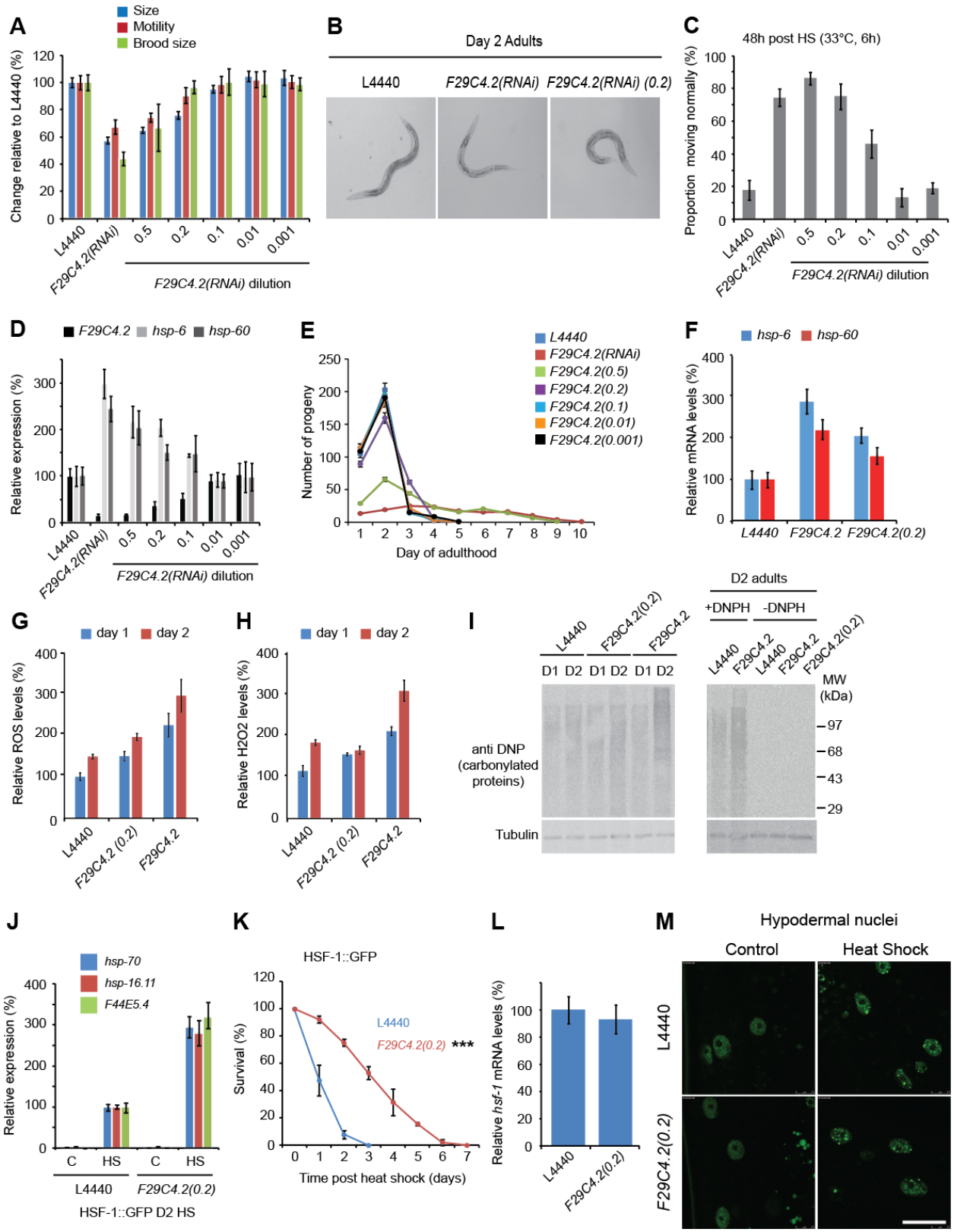

Supplemental figure 3, related to main figure 3. *F29C4.2* knockdown influences animal physiology and stress resistance in a dose dependent manner

(A and B) Relative (A) size, motility (body lengths per second), and total brood size with (B) representative brightfield images of worms on day 2 of adulthood. Brood size values are the mean of at least 20 animals. Error bars denote SEM.

(C) Thermorecovery of N2 worms grown on L4440, *F29C4.2(RNAi)*, or *F29C4.2(RNAi)* diluted 2, 5, 10, 100, and 1000 fold with L4440, 48 hours post heat shock at 33°C for 6 hours on day 2 of adulthood. Values are the mean of 4 biological replicates. Bars represent SEM.

(D) *F29C4.2*, *hsp-6*, and *hsp-60* mRNA levels at day 2 of adulthood in animals grown on L4440 or *F29C4.2(RNAi)* diluted 2, 5, 10, 100, and 1000 fold with L4440. Values are the mean of 4 biological replicates.

(E) Number of progeny produced during adulthood in animals grown on L4440, *F29C4.2(RNAi)*, or *F29C4.2(RNAi)* diluted 2, 5, 10, 100, or 1000 fold. Values are the mean of 20 animals and bars represent SEM.

(F) Relative *hsp-6* and *hsp-60* expression at day 2 of adulthood in L4440, *F29C4.2*, or *F29C4.2(0.2)* animals. Values were calculated relative to the housekeeping genes *rpb-2* and *cdc-42* and are the mean of 4 biological replicates. Bars represent SEM.

(G) Levels of general ROS measured by dihydroxyethidium (DHE) oxidation on day 1 and day 2 of adulthood in animals grown on L4440, *F29C4.2*, or *F29C4.2(0.2)(RNAi)*. Values are the mean of biological replicates and bars denote SEM.

(H) Relative hydrogen peroxide (H_2O_2) levels at day 1 and day 2 of adulthood in L4440, *F29C4.2*, or *F29C4.2(0.2)(RNAi)* animals as measured by amplex-red fluorescence assay. Values are the mean of biological replicates and bars denote SEM.

(I) Representative western blots of levels of carbonylated proteins at day 1 and day 2 of adulthood in L4440, *F29C4.2*, or *F29C4.2(0.2)(RNAi)* animals. Tubulin was probed as a loading control and - DNPH samples demonstrate specificity of the anti-DNP antibody.

(J) Relative expression of canonical HSR genes in HSF-1::GFP (AM1060) worms exposed to control or heat shock (33°C, 30 min) conditions at day 2 of adulthood. Values were calculated relative to the housekeeping genes *rpb-2* and *cdc-42* and are the mean of 4 biological replicates. Bars represent SEM.

(K) Survival of HSF-1::GFP worms at different days of recovery following 35°C heat shock for 4 hours on day 2 of adulthood. Values and are the mean of 4 biological replicates and bars represent SEM. Statistical significance was calculated by TWO-WAY ANOVA with Bonferroni correction. *** = $p < 0.001$.

(L) Relative *hsf-1* mRNA levels on day 2 of adulthood in L4440, *F29C4.2*, or *F29C4.2(0.2)(RNAi)* treated animals. Values were calculated relative to the housekeeping genes *rpb-2* and *cdc-42* and are the mean of 4 biological replicates. Bars represent SEM.

(M) Representative images of hypodermal nuclei of HSF-1::GFP worms grown on L4440 or *F29C4.2(0.2)(RNAi)* and exposed to control or HS conditions on day 2 of adulthood.

Supplemental Figure 4

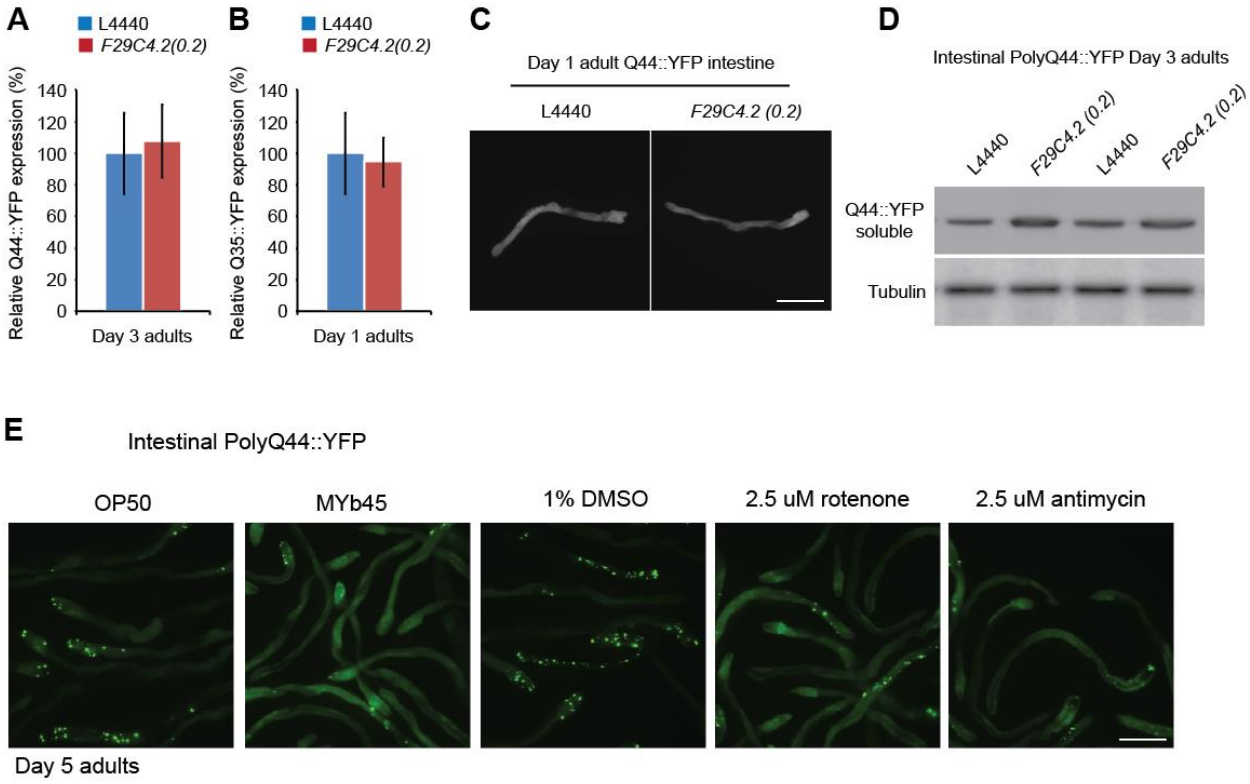

Supplemental figure 4, related to main figure 4. *F29C4.2(0.2)(RNAi)* does not alter expression of polyglutamine transgenes

(A) Relative expression of polyQ(44)::YFP mRNA at day 3 of adulthood in L4440 and *F29C4.2(0.2)(RNAi)* treated animals. Values are the mean of 4 biological replicates and error bars denote SEM.

(B) Relative expression of polyQ(35)::YFP mRNA at day 1 of adulthood in L4440 and *F29C4.2(0.2)(RNAi)* treated animals. Values are the mean of 4 biological replicates and error bars denote SEM.

(C) Representative fluorescence images of day 1 adult worms expressing polyQ(44)::YFP in the intestine following growth on L4440 or *F29C4.2(0.2)(RNAi)*. Scale bar = 250 µM.

(D) Western blots of soluble polyQ(44)::YFP and tubulin levels in day 3 adults following growth on L4440 or *F29C4.2(0.2)(RNAi).*

(E) Representative images of *vha-6p*::polyQ(44)::YFP animals at day 5 of adulthood following exposure to vehicle (1% DMSO), 2.5 uM rotenone, 2.5 uM antimycin, OP50 or MYb45. Scale bar = 250 µM.

Supplemental Figure 5

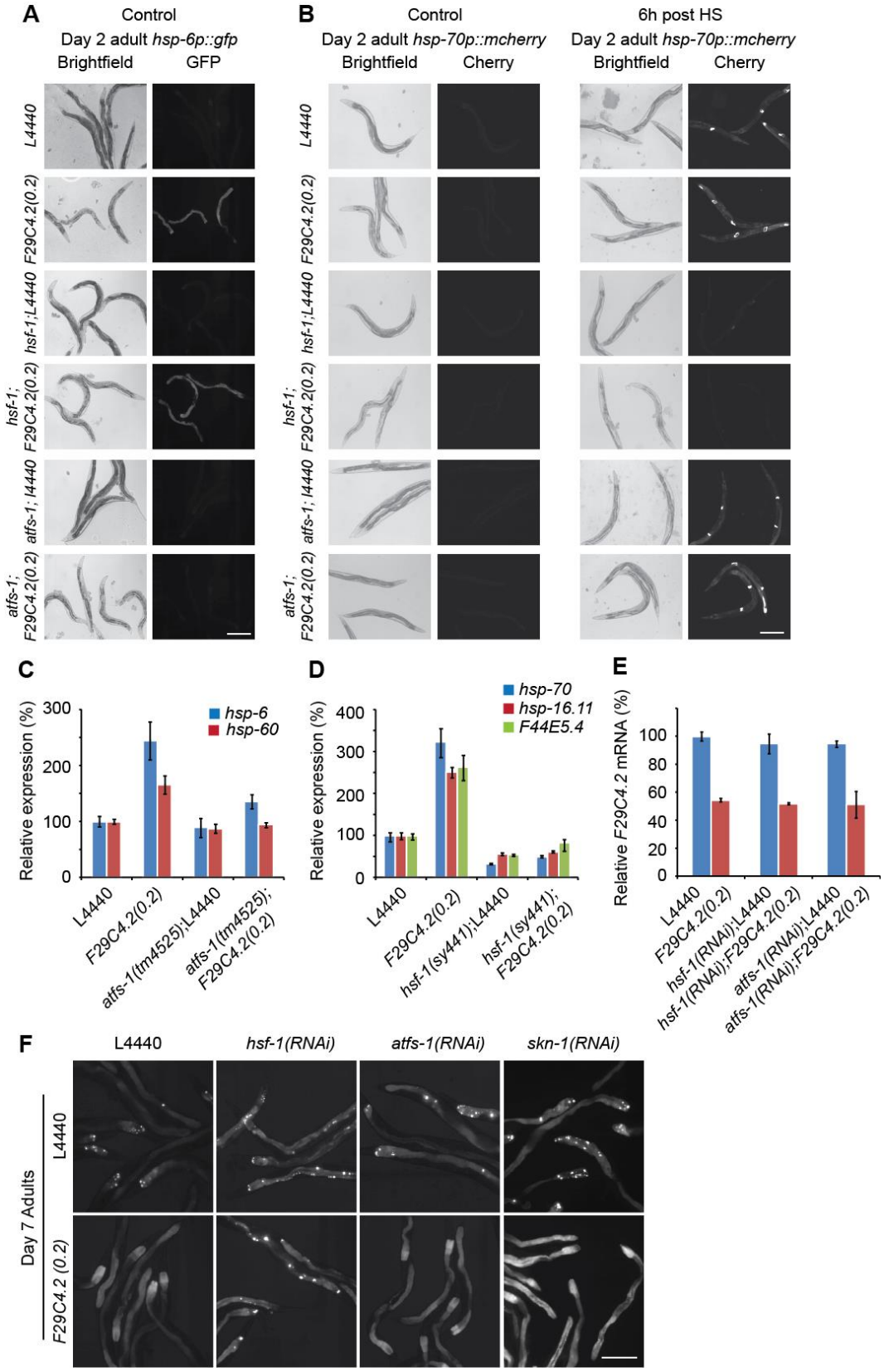

Supplemental figure 5, related to main figure 5. Combinatorial RNAi with *atfs-1(RNAi)* or *hsf-1(RNAi)* suppresses the UPR^{mt} and HSR respectively but does not impair *F29C4.2* knock-down

(A) Representative brightfield and fluorescence images of animals expressing *hsp-6p*::gfp under control conditions following growth on L4440, *F29C4.2(0.2)*, *hsf-1*;L4440, *hsf-1;F29C4.2(0.2)*, *atfs-1*;L4440, or *atfs-1;F29C4.2(0.2)* RNAi. Scale Bar = 250 µM.

(B) Representative brightfield and fluorescence images of animals expressing *hsp-70p*::mCherry under control conditions or 24 hours post heat shock (HS) following growth on L4440, *F29C4.2(0.2)*, *hsf-1*;L4440, *hsf-1;F29C4.2(0.2)*, *atfs-1*;L4440, or *atfs-1;F29C4.2(0.2)* RNAi. Scale Bar = 250 µM.

(C) Relative expression of *hsp-6* and *hsp-60* on day 2 of adulthood in wild type or *atfs-1(tm4525)* mutants following growth on L4440 or *F29C4.2(0.2)(RNAi).*

(D) Relative expression of *hsp-70, hsp-16.11, and F44E5.4* in wild type or *hsf-1(sy441)* mutants following heat shock on day 2 of adulthood after growth on L4440 or *F29C4.2(0.2)(RNAi).*

(E) Relative expression of *F29C4.2* at day 2 of adulthood in animals grown on L4440, *F29C4.2(0.2)*(RNAi), *hsf-1*;L4440, *hsf-1;F29C4.2(0.2)*, *atfs-1*;L4440, or *atfs-1;F29C4.2(0.2)* RNAi.

(F) Representative images of the intestine of worms expressing Q44::YFP (*vha-6::polyQ(44)::YFP*) on day 7 of adulthood following growth on L4440, *F29C4.2(0.2)*, *hsf-1*;L4440, *hsf-1;F29C4.2(0.2)*, *atfs-1*;L4440, *atfs-1;F29C4.2(0.2)* RNAi, *skn-1*;L4440, or *skn-1;F29C4.2(0.2)* RNAi. Scale bar = 250 µM.

Supplemental Table 1, related to main figure 1: Suppressors of thermorecovery in early adulthood

Gene	Human ortholog	Function
F29C4.2	*COX6C*	ETC complex IV
mtch-1	*MTCH1/MTCH2*	Mitochondrial carrier protein
C50F2.3	*XAB2*	Splicing factor
dct-19	*EPHX1*	Epoxide hydrolase
tba-8	*TUBA8*	Alpha tubulin
B0024.11	*PUS7*	Pseudouridine synthase
ubxn-6	*UBXN6*	Ubiquitin domain containing protein
slc-25A26	*SLC25A26*	S-adenosylmethionine transporter
twk-22	*KCNK10*	Potassium channel protein
dnj-7	*DNAJC3*	ER DNAJ chaperone
C53B4.4	*PDZD8*	Unknown

Supplemental Table 2, related to experimental procedures: Summary of primer pairs used in this study

Target	**Forward**	**Reverse**
hsp-70(C12C8.1)	CTACATGCAAAGCGATTGGA	GGCGTAGTCTTGTTCCCTTC
hsp-16.11	GGCTCAGATGGAACGTCAA	GCTTGAACTGCGAGACATTG
hsp-70(F44E5.4)	TGATACCCATCTCGGAGGAG	GTGGATTGGGTGAAATGTCC
rpb-2	AACTGGTATTGTGGATCAGGTG	TTTGACCGTGTCGAGATGC
cdc-42	GGTTGCTCCAGCTTCATTC	AACAAGAATGGGGTCTTTGA
hsp-4	GGGGACAATCATTGGTATCG	ACGCAACGTATGATGGAGTG
hsp-6	GTTATCGAGAACGCAGAAGGAG	CATCCTTAGTAGCTTGACGCTG
hsp-60	CATGCTCGTCGGAGTCAAC	TTTGTGATCTTTGGGCTTCC
gst-4	GCTACTTGGATAACCAGCTCCA	TCGTCTGGCATCAAAGAACAGT
F29C4.2	AAGACTGTTGCCGATTTGTAG	TTACGAACATTTTTATTCGGAACA
hsf-1	TGTACAAGGACGTCCCGAAT	TCCAAATTTTGTTGCGTCTG
daf-21	GACCAGAAACCCAGACGATATC	GAAGAGCACGGAATTCAAGTTG
hsp-1	ACTTCTACACCAACATCACTCG	CAAGGACGATGTCATGAACTTG
hsp-70 promoter	ATAGCATAGGCGACCCACAG	ACGTTCCTCTGGCATCTTCT
hsp-16.11 promoter	CTGAATGTGAGTCGCCCTCC	GAGAGCCTCTGCAAACTGGA
F44E5.4 promoter	CCAGCTGCATCACTCTGTCT	GGCCGACAGAAGAGACAACA
cdc-42 promoter	GTAAAGAAACGCTCGTGGCA	GATCGTCTGCATTTCGCCTG